



## THESIS APPROVAL

### GRADUATE SCHOOL, KASETSART UNIVERSITY

Master of Science (Biotechnology)

**DEGREE**

Biotechnology

**FIELD**

Biotechnology

**DEPARTMENT**

**TITLE:** Bacterial Cellulose Filled Natural Rubber Composites

**NAME:** Miss Walaiporn Rungjang

**THIS THESIS HAS BEEN ACCEPTED BY**

**THESIS ADVISOR**

( Mr. Prakit Sukyai, Dr.nat.techn. )

**THESIS CO-ADVISOR**

( Miss Rattana Tantatherdtam, Ph.D )

**DEPARTMENT HEAD**

( Associate Professor Suttipun Keawsompong, Ph.D )

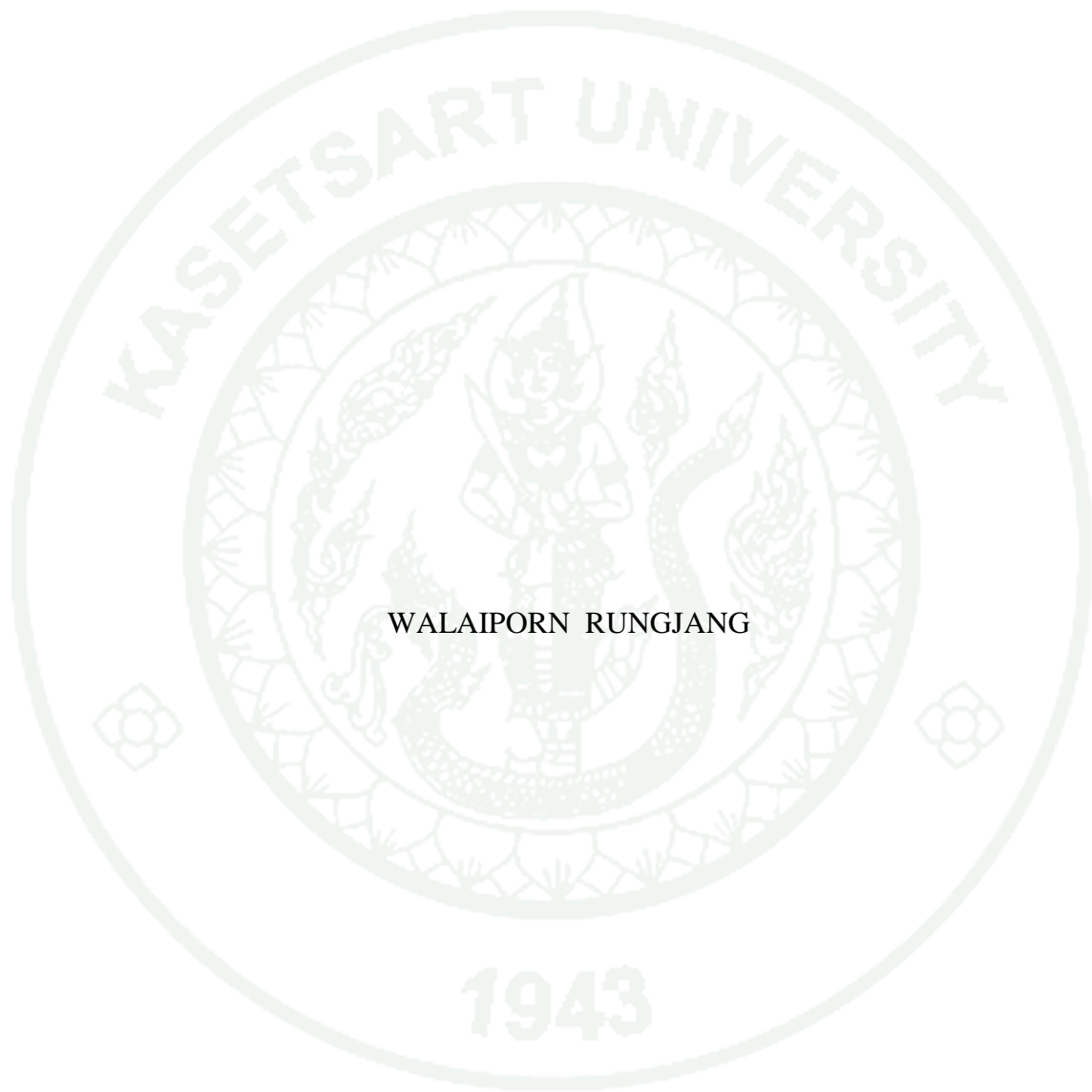
**APPROVED BY THE GRADUATE SCHOOL ON** \_\_\_\_\_

**DEAN**

( Associate Professor Gunjana Theeragool, D.Agr. )

THESIS

BACTERIAL CELLULOSE FILLED NATURAL RUBBER  
COMPOSITES



WALAIPORN RUNGJANG

A Thesis Submitted in Partial Fulfillment of  
the Requirements for the Degree of  
Master of Science (Biotechnology)  
Graduate School, Kasetsart University  
2013



Walaiporn Rungjang 2013: Bacterial Cellulose Filled Natural Rubber Composites. Master of Science (Biotechnology), Major Field: Biotechnology, Department of Biotechnology. Thesis Advisors: Mr. Prakit Sukyai, Dr.nat.techn. 70 pages.

Bacterial cellulose (BC) produced by the *Glucanacetobacter xylinus* and the BC powder was produced from dried BC by mechanical process. The particle size of BC powder was in approximately 180  $\mu\text{m}$ . It was used as reinforcing element in natural rubber matrix and a source of bacterial cellulose nanowhiskers (BCNWs) extraction. BCNWs were produced from BC using sulfuric acid hydrolysis. The average length (L) and diameter (D) of BCNWs were 186 nm and 7 nm, respectively, giving an aspect ratio (L/D) around 28. The BCNWs were used as reinforcing phase to nanocomposites films using latex of natural rubber as matrix. Natural rubber (NR) reinforce BC composites were prepared on a laboratory two-roll mill. The influences of BC concentration on the cure characteristics, mechanical and thermal properties of the rubber composites were investigated. The scorch time decreased with an increase in cellulose loading, but there was no appreciable change in cure time. A significant improvement of modulus and hardness was observed as a result of the addition of BC to the NR matrix, especially at high cellulose loading, while the tensile strength and elongation at break of natural rubber composites decreased with increasing BC filler loading. Differential scanning calorimetry (DSC) and dynamic mechanical analysis (DMA) results showed no change in the glass transition temperature ( $T_g$ ) of the rubber matrix with the addition of BC, but there was a softening of rubber. DMA showed the stiffness and rigidity of composites. Scanning electron microscopy (SEM) revealed the morphology of bacterial cellulose and the interaction between matrix and cellulose. The effect of BCNWs loading on tensile and thermal properties was investigated. Both tensile strength and modulus showed improved stiffness for bacterial cellulose nanowhiskers/natural rubber (BCNWs/NR) nanocomposites at 7.5% BCNWs loading. On the other hand, elongation at break of BCNWs/NR nanocomposites was decreased with increasing BCNWs filler loading. Differential scanning calorimetry results exhibited no change in  $T_g$ . The thermogravimetric analysis indicated that no significant effect of the BCNWs on degradation temperature of NR whereas the onset temperature was slightly changed.

---

Student's signature

---

Thesis Advisor's signature

## ACKNOWLEDGEMENTS

I would like to send my deepest appreciation to my advisor, Dr. Prakrit Sukyai for his invaluable guidance and encouragement throughout this study. I would also gratefully thank co-advisor Dr. Rattana Tantatherdtam for her generosity, guidance, improvement and encouragement throughout this work. My thanks also go to my representative of graduate school Dr. Jackapon Sunthornvarabhas for their comments and suggestion. My sincere thanks are also to Dr. Wanticha Labsiri for their unlimited help and kind encouragement.

I would like to thank you to all my friends Tarn, P Pong, Benz, Porz, Tang, Kim, Ploy, Vo, P Fay, P Kob, P Jamp, P Keaw, P Por for their unlimited help and to everyone that their names are not mentioned here but I fully know in my heart. Most of all, I would like to thank all the unconditional love and support from my family that helped me to get through all the difficulties.

Walaiporn Rungjang

April 2013

## TABLE OF CONTENTS

	<b>Page</b>
TABLE OF CONTENTS	i
LIST OF TABLES	ii
LIST OF FIGURES	iii
INTRODUCTION	1
OBJECTIVES	3
LITERATURE REVIEW	4
MATERIALS AND METHODS	29
Material	29
Methods	31
RESULTS AND DISCUSSION	37
CONCLUSION	58
LITERATURE CITED	59
CURRICULUM VITAE	70

## LIST OF TABLE

Table	Page
1 Properties of plant (PC) and bacterial (BC) cellulose	11
2 Typical infrared absorption frequencies for bacterial cellulose.	12
3 I / I <sub>0</sub> ratio for different cellulose sources	13
4 Mechanical properties of BC and other organic layer material	14
5 Examples of applications of bacterial cellulose	15
6 Formulation of the NR/BC Composites	32
7 Degradation onset temperature (T <sub>o</sub> ), peak degradation temperature (T <sub>max</sub> ) and corresponding weight loss (WL) of native bacterial cellulose (BC) and nanowhiskers (BCNWs).	42
8 Curing characteristics and mechanical properties of natural rubber and natural rubber/bacterial cellulose composites.	44
9 Glass transition temperature of bacterial cellulose/natural rubber composites from differential scanning calorimeter	47
10 Peak height and Tg from tan $\delta$ of bacterial cellulose/natural rubber composites	50
11 Tensile properties of the nanocomposites in comparison with matrix	53

## LIST OF FIGURES

Figure		Page
1	Simplified pathways of carbon metabolism in <i>Acetobacter xylinum</i>	5
2	Schematic illustration of BC biogenesis and fibril formation	6
3	BC pellicle formed in static culture	7
4	BC pellets formed in agitated culture	7
5	Scanning electron micrographs of BCs produced in agitated and static cultures. (a) BC reticulated structure in gelatinous membrane produced in the static culture (b) BC reticulated structure in granules accumulated in the agitated culture	9
6	The -1,4 glucosidic linkage of BC unit chain	10
7	Outline of intra- and inter molecular hydrogen bonds among cellulose chains	10
8	DSC thermogram of a BC membrane. The temperatures at D and B refer to the dehydration (87°C) and burning (363°C) peak temperatures, respectively.	14
9	Classification of fiber reinforced composites	16
10	Position of hydroxyl groups on cellulose backbone	21
11	Forming charged surface sulfate ester group of cellulose nanowhiskers	23
12	Acid hydrolysis breaks down disordered (amorphous) regions and isolates nanocrystals.	24
13	The structure of cis-1,4 polyisoprene	25
14	Image of (a) BC and (b) BC powder	37
15	TEM micrograph of nanowhiskers (BCNW)	38
16	AFM images of bacterial cellulose nanocrystals obtained after acid hydrolysis treatment (a) Height Images and (b) Phase images	39
17	X-ray diffraction pattern of native bacterial cellulose (BC) and nanowhiskers (BCNW)	40



## LIST OF FIGURES (Continued)

Figure		Page
18	FTIR spectra of native bacterial cellulose (BC) and nanowhiskers (BCNW)	41
19	TG curves of BC and BCNWs	42
20	Typical stress-strain curves obtained from tensile test for NR vulcanizate and BC/NR composites	46
21	Storage modulus ( $E'$ ) versus temperature curve at 1 Hz of BC/NR composites	47
22	Tan $\delta$ versus temperature curve at 1 Hz of bacterial cellulose/natural rubber composites	49
23	SEM photograph of fracture surface of the natural rubber reinforce with 5, 10, 15 and 20 phr bacterial cellulose at magnification of 350X : (A) 5 phr (B) 10 phr (C) 15 phr (D) 20 phr	51
24	Typical stress-strain curves obtained from tensile test for BCNWs/NR nanocomposites	53
25	DSC thermograms of NR and BCNWs/NR nanocomposites	54
26	TGA curve of neat NR and BCNWs/NR nanocomposites reinforcement with 2.5, 5, 7.5, 10 and 15% (wt%) BCNWs	56
27	DTG curve of neat NR and BCNWs/NR nanocomposites reinforcement with 2.5, 5, 7.5, 10 and 15% (wt%) BCNWs	56
28	SEM of fracture surfaces of NR base films reinforced with BCNWs : (a) neat NR (b) NR-BC2.5 (c) NR-BCNWs10 (d) NR-BCNWs15	57

# BACTERIAL CELLULOSE FILLED NATURAL RUBBER COMPOSITES

## INTRODUCTION

Bacterial cellulose (BC) is produced by bacteria belonging to genus *Gluconacetobacter*, *Sarcina*, and *Agrobacterium* (Trovatti *et al.*, 2011). From the culture medium, a pure-cellulose network free of lignin and hemicellulose is obtained as highly hydrated pellicles, composed of a random assembly of ribbon-shaped fibers less than 100 nm wide (Barud *et al.*, 2011). Hence, no chemical treatments are needed to remove lignin and hemicelluloses, as is the case for plant cellulose (Lee *et al.*, 2012). In terms of chemical structure, bacterial cellulose is identical to that produced by plants. However, it exhibits high crystallinity, water-holding capacity, degree of polymerization, and mechanical strength and purity (Sheykhnazari *et al.*, 2011). The bacterial cellulose can be easily processed into microfibrils, nanofibrils and nanocrystals through a top-down approach which are useful as reinforcing components in the preparation of polymer nanocomposites for high performance applications (George *et al.*, 2011).

For their application as nanofillers, cellulosic materials are usually subjected to hydrolysis with strong acids such as sulfuric acid, which produce a preferential digestion of the amorphous domains of the material and cleavage of the nanofibril bundles (Rånby *et al.*, 1949), therefore breaking down the hierarchical structure of the material into crystalline nanofibres or nanocrystals, usually referred to as cellulose nanowhiskers (CNWs) (Martinez-Sanz *et al.*, 2011). Cellulose nanowhiskers has high stiffness, surface area and crystallinity are suitable for applications in polymeric matrices, acting as reinforcing elements (Teixeira *et al.*, 2011) which in some cases contributes to enhance the rigidity but mostly embrittles the polymer (Bras *et al.*, 2010).



Natural rubber (NR) is a high molecular weight polymer of isoprene (2-methyl 1,3-butadiene) and is the oldest known rubber (Visakh *et al.*, 2012). In any case, some properties of natural rubber such as modulus, hardness and abrasion resistance need to be improved for some specific applications (Zhang *et al.*, 2010). Various natural fibers have been used as reinforcement in NR such as sisal (Jacob *et al.*, 2004; Jacob *et al.*, 2010), short-isora-fiber (Mathew and Joseph, 2007), bamboo fiber (Ismail *et al.*, 2002), grass fiber (De *et al.*, 2004), pineapple leaf fiber (Lopattananon *et al.*, 2006), oil palm fiber (Joseph *et al.*, 2010), cassava bagasse cellulose whiskers (Pasquini *et al.*, 2010), sugar cane bagasse cellulose whiskers (Bras *et al.*, 2010), capim dourado and sisal cellulosic nanoparticles (Siqueira *et al.*, 2010b). Hence, bacterial cellulose fibers would be able to use as reinforcing fillers in rubbers.

According to the literature survey, they were lack of utilization of BC as reinforcing filler in NR. Therefore, it is our interest to study the evaluation of curing characteristics, mechanical properties, thermal properties of NR vulcanizate by using BC powder as reinforcing agent. Moreover, BCNWs were prepared by using acid hydrolysis and used as nanofillers in NR latex. The influence of BCNWs loading on mechanical and thermal properties of nanocomposites films were investigated.

## OBJECTIVES

The objectives of this study are:

1. To study the utilization of bacterial cellulose powder and bacterial cellulose nanowhiskers as reinforcing agents in natural rubber.
2. To investigate the influence of bacterial cellulose powder and bacterial cellulose nanowhiskers on thermal, mechanical and chemical properties of natural rubber composites.

## LITERATURE REVIEW

### 1. Bacterial cellulose (BC)

Bacterial cellulose (BC), an exopolysaccharide, is produced by many species of bacteria, such as those in the genera of *Acetobacter*, *Agrobacterium*, *Achromobacter*, *Aerobacter*, *Azotobacter*, *Sarcina ventriculi*, *Salmonella*, *Escherichia* and *Rhizobium* (Sheykhnazari *et al.*, 2011). In particular *Gluconacetobacter xylinus* bacteria produces cellulose markedly different from plant cellulose. From the culture medium, a pure-cellulose network free of lignin and hemicellulose is obtained as highly hydrated pellicles, composed of a random assembly of ribbon-shaped fibers less than 100nm wide (Barud *et al.*, 2011). BC is becoming a promising biopolymer for several applications, including nanocomposite materials, due to its unique properties, such as high crystallinity, high mechanical strength, ultra-fine nanofibrillar network structure and high purity (Trovatti *et al.*, 2010).

#### 1.1 Biosynthesis of BC

BC is produced extracellularly by bacteria of the genus *Gluconacetobacter* (formerly *Acetobacter*). This is a gram-negative bacterium, strictly aerobic, capable of producing cellulose extracellularly at temperatures between 25 and 30 °C and pH from 3 to 7 using glucose, fructose, sucrose, mannitol, among others, as carbon sources (Pecoraro *et al.*, 2008). The biosynthesis of BC is a precisely and specifically regulated multi-step process, involving a large number of both individual enzyme and complexes of catalytic and regulatory proteins, whose supramolecular structure has not yet been well defined. The process includes the synthesis of uridine diphosphoglucose (UDPGlc), which is cellulose precursor, followed by glucose polymerization into the  $\alpha$ -1,4-glucan chain, and nascent chain association into characteristic ribbon-like structure, formed by hundred or even thousands of individual cellulose chains (Park *et al.*, 2009), as show in figure 1.

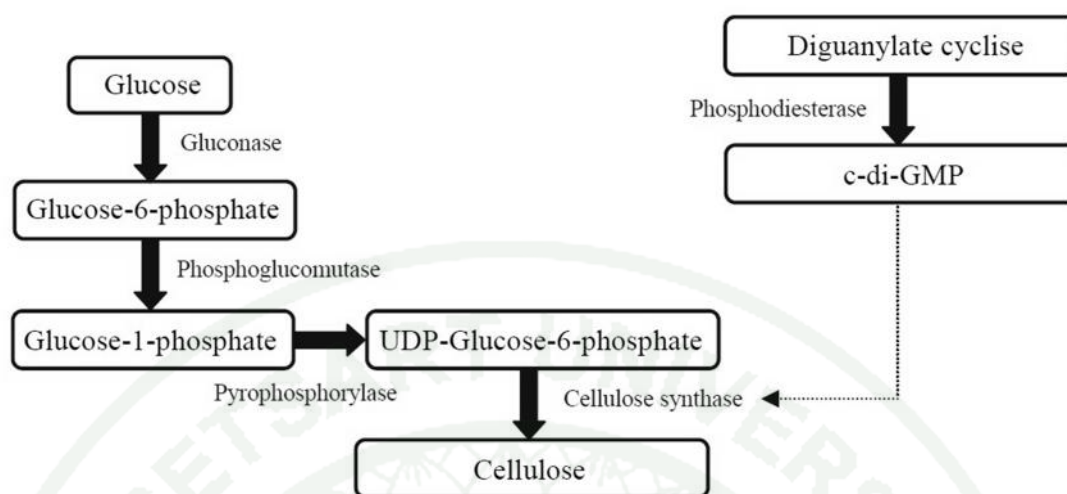


**Figure 1** Simplified pathways of carbon metabolism in *Acetobacter xylinum*.

**Source:** Quéro (2011)

BC is synthesized in three stages. In the first stage, glucose molecules are polymerized (formation of  $\alpha$ -1,4-glucosidic linkages) between the outer and cytoplasm membranes, forming cellulose chain (Pecoraro *et al*, 2008). The chain exits the cell as a so-called *elementary fibril* through pores at the bacterium surface (Klemm *et al.*, 2006). The cellulose chains that group with another 36 chain to form an elementary fibril, which has a diameter of approximately 3.5 nm. About 46 adjacent fibrils join through hydrogen bonds to form a ribbon, which has a width ranging from 40 to 60 nm. The ribbons roll up to form the fibre, which gets tangled with the other fibres dispersed in the culture medium. The entangled fibres form a jelly-like film on the surface of the liquid culture medium. The film containing the bacteria is called *zooglea*. Its thickness depends on the cultivation time and can usually reach 1 or 2 cm. Each extrusion pore bears a site for cellulose chains production called terminal complex (TC) (figure 2) and each TC accomplishes several different processes, all controlled genetically within the biosynthetic route. Many studies have been undertaken for both plant and bacterial cellulose, in order to find the proteins, enzymes and to map the genes that are involved in each synthesis step, but, until now, none is conclusive (Pecoraro *et al*, 2008).

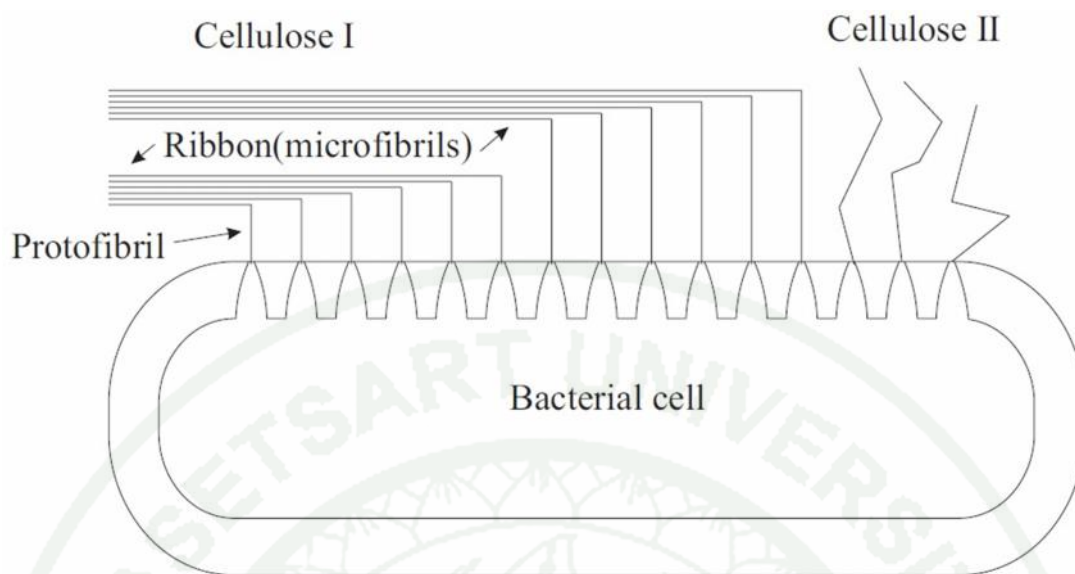


**Figure 2** Schematic illustration of BC biogenesis and fibril formation.

**Source:** Staiger *et al.* (2007)

The macroscopic morphology of bacterial cellulose depends on the conditions of culturing. In static conditions (Figure 3), bacteria accumulate a cellulose “pellicle” on the surface of a nutrient broth at the oxygen-rich air/liquid interface. Protofibrils of cellulose are continuously extruded from linearly ordered pores at the surface of the bacterial cell, crystallized into microfibrils and forced deeper into the growth medium. The leather-like pellicle, supporting the population of *Acetobacter xylinum* cells, consists of overlapping and inter-twisted ribbon like cellulose microfibrils, forming parallel but disorganized planes. Under agitated culture conditions (Figure 4) bacterial cellulose is produced as a well-dispersed slurry of irregular masses including granules, stellate and fibrous strands (Bielecki *et al.*, 2002).





**Figure 3** BC pellicle formed in static culture.



**Figure 4** BC pellets formed in agitated culture.

**Source:** Bielecki *et al.* (2002)

The fibrils of BC produced statically were more highly extended (Fig. 5a). In contrast, the fibrils of bacterial cellulose produced under agitated conditions were curved and entangled with each other resulting in a denser reticulated structure than those of static culture (Fig. 5b) (Watanabe *et al.*, 1998). The culturing of the bacteria under static conditions normally takes place at 28–30°C by adding an aliquot of activated seed broth to the culture medium in a vessel such as beaker. Initially, the system becomes turbid. After a period, a white pellicle begins to form on the surface, increasing in thickness with time. After harvesting the BC is purified by boiling it in 1% NaOH for 2 hr, treating with 5% acetic acid and then thoroughly washing in distilled water until the pellicle becomes transparent (Haiyuan, 2006).

## 1.2 Structure and properties of BC

Cellulose is an unbranched polymer of  $\beta$ -1,4-linkage glucopyranose residues, as shown in Figure 6 (Park *et al.*, 2009). Extensive research on BC revealed that it is chemically identical to plant cellulose, but its macromolecular structure and properties differ from the latter (Bielecki *et al.*, 2002). Micro-fibril diameters of BC are about 24-86 nm and 72-175 nm (Gindl and Keckes, 2004). The cellulose chains interact through hydrogen bond, assuming a parallel orientation among them. The structure and rigidity of BC is provided by the OH intra and intermolecular hydrogen bond, as shown in Figure 7 (Pecoraro *et al.*, 2008).



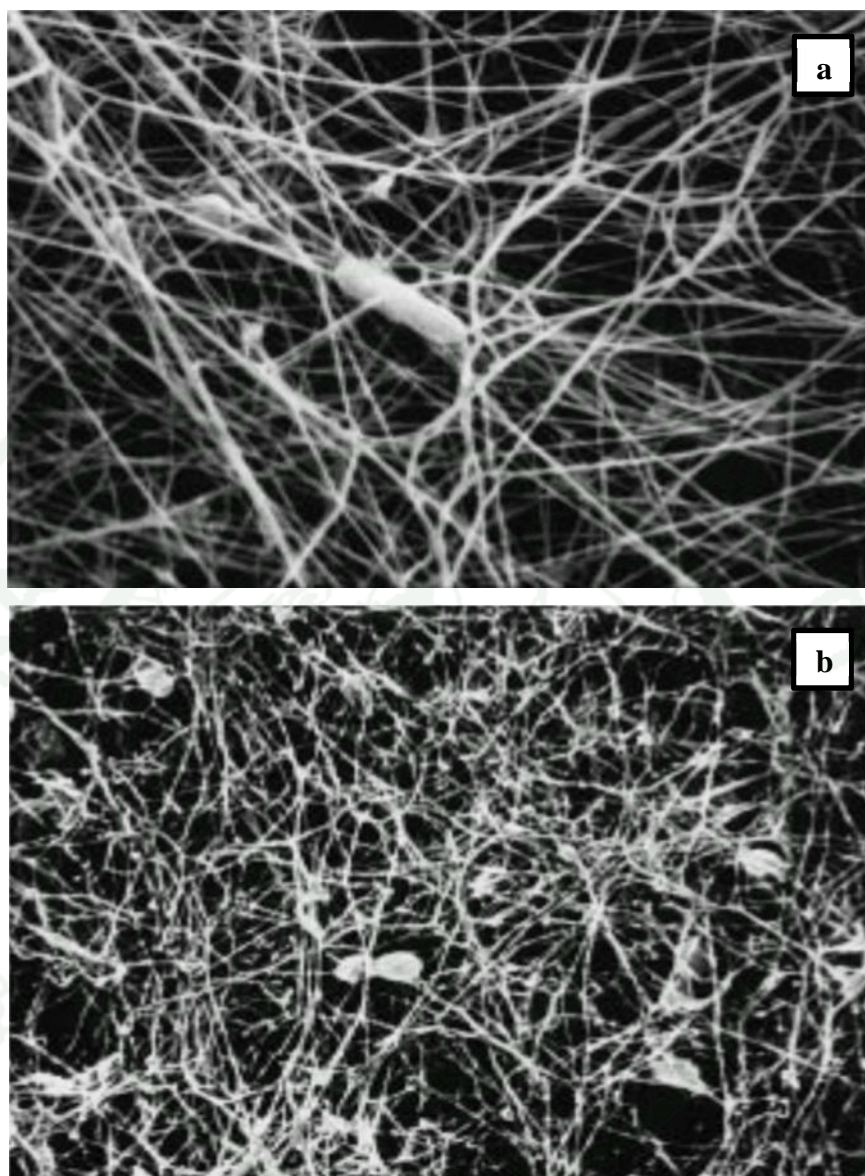


**Figure 5** Scanning electron micrographs of BCs produced in agitated and static cultures. (a) BC reticulated structure in gelatinous membrane produced in the static culture (b) BC reticulated structure in granules accumulated in the agitated culture.

**Source:** Watanabe *et al.* (1998)

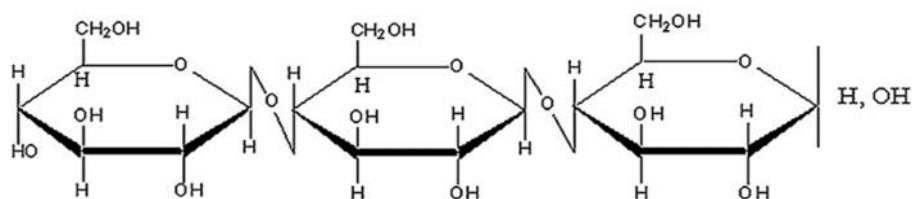


**Figure 6** The  $\beta$ -1,4 glucosidic linkage of BC unit chain.

**Source:** Pecoraro *et al*, 2008

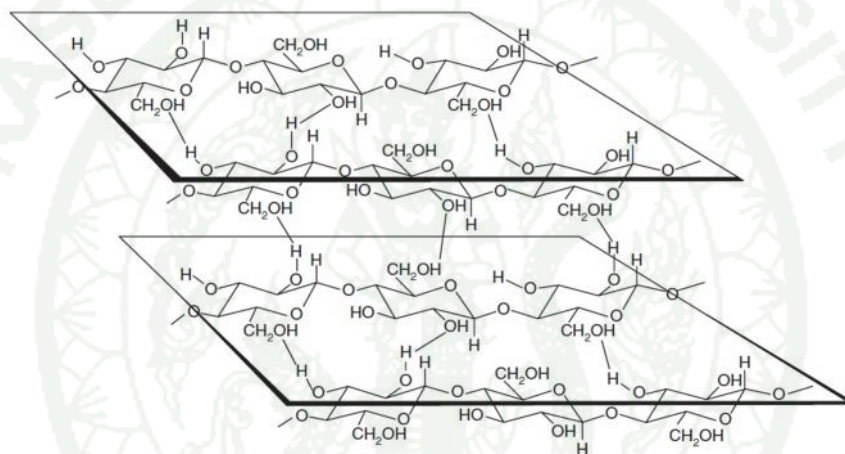


**Figure 7** Outline of intra- and inter molecular hydrogen bonds among cellulose chains.

**Source:** Pecoraro *et al*, 2008

BC is also distinguished from its plant counterpart by a high crystallinity index (above 60%) and different degree of polymerization (DP), usually between 2,000 and 6,000, but in some cases reaching even 16,000 or 20,000 (Watanabe *et al.*, 1998), whereas the average DP of plant polymer varies from 13,000 to 14,000 (Bielecki *et al.*, 2002). Moreover, the macromolecular structure and properties of BC also differ from the latter (Park *et al.*, 2009). Some properties of vegetal and BC are shown in Table 1.

**Table 1** Properties of plant cellulose (PC) and BC

Properties	Plant cellulose	BC
Fibre width	$1.4-4.0 \times 10^{-2}$ mm	70-80 nm
crystallinity	56-65 %	65-79%
Degree of polymerization	13,000-14,000	2,000-6,000
Young's modulus	5.5-12.6 GPa	15-30 GPa
Water content	60 %	98.5 %

**Source :** Pecoraro *et al.* (2008)

Native BC occurs in two different crystalline structure, namely cellulose I $\alpha$  and cellulose I $\beta$ . A triclinic unit cell consisting of one cellulose chain for cellulose I $\alpha$  and a monoclinic unit cell consisting of two cellulose chain for cellulose I $\beta$ . These two types of crystalline structures appear to be separated distributed in the microfibril of cellulose with exception of tunicin (sea squirt cellulose) which is pure cellulose I $\beta$ . Cellulose I $\alpha$  is dominant in BC while cellulose I $\beta$  is dominated in plant cellulose (Park *et al.*, 2009).

### 1.2.1 Vibrational spectroscopy

The functional groups that characterize BC are the same as those of vegetable cellulose and the corresponding peaks are assigned in Table 2. The native BC exist in two different crystalline structure, i.e., cellulose I $\alpha$  and cellulose I $\beta$  (Yoshinaga *et al.*, 1997). Infrared spectroscopy can also be used for the determination of the I $\alpha$ /I $\beta$  ratio. The method is based on the difference in the stretching energies, and the peaks, assigned to the OH groups present in each phase. The peak at 750 cm<sup>-1</sup> corresponds to the triclinic phase (I $\alpha$ ), while that at 710 cm<sup>-1</sup> is attributed to monoclinic phase (I $\beta$ ). Hence, the ratio between the area under these peaks gives the ratio between the phases. The I $\alpha$ /I $\beta$  ratio shows variations related to the origin of

cellulose. Algae and bacteria forms are rich in triclinic phase (I<sub>1</sub>), while higher plants are rich in monoclinic phase (I<sub>2</sub>) (Pecoraro *et al.*, 2008).

**Table 2** Typical infrared absorption frequencies for BC.

Rang (cm <sup>-1</sup> )	Assignment <sup>a</sup>
3,500-3,300	ν OH
3,000-2,870	ν CH and CH <sub>2</sub> (CHOH; CH <sub>2</sub> OH)
1,645	s HOH
1,430-1,330	C-OH e CH
1,200-1,000	ν C-O (-C-O-H)
1,150-1,000	ν C-O (C-O-C)
900-700	as in plane CH <sub>2</sub> C-H
700-400	out of the plane OH

<sup>a</sup> ν = stretching; = angular bending; s = symmetric; as = asymmetric.

**Source:** Pecoraro *et al.* (2008)

Table 3 shown the ratio between the I<sub>1</sub> and I<sub>2</sub> phases depends on the cellulose source. The content of cellulose I<sub>1</sub> is approximately 60% in BC while it is only approximately 30% in the higher plant cellulose, cotton and ramie. In contrast, cellulose I<sub>2</sub> is the major component in plant cellulose. Crystallinity is considered to be a key determinant of properties of cellulose (Park *et al.*, 2009).



**Table 3** I / I ratio for different cellulose sources.

Type	Class	Ratio I / I (%)
Glucanoacetobacter	Bacterial	64/36
Valonia	Vegetal (algae)	60/40
Halocynthia	Animal	10/90

**Source:** Pecoraro *et al.* (2008)

### 1.2.2 Mechanical strength

The mechanical properties of BC are great. The Young's modulus and tensile strength are 16.9 GPa and 256 MPa, respectively. In comparison, the Young's modulus and tensile strength of cotton linter paper is 0.085 GPa and 0.83 MPa, respectively. The high mechanical properties of BC film are ascribed to its microstructure. The microfibrils are bound through interfibrillar hydrogen bonds, as in pulp-paper. However, the density of the interfibrillar hydrogen bonds is higher since the microfibrils are much finer leading to a greater contact area. The mechanical properties of single fibers of BC was measured by Atomic Force Microscopy, and a Young's modulus was determined as  $78 \pm 17$  GPa (Haiyuan, 2006). Table 4 describes the mechanical properties of BC and other organic layer materials. Due to this remarkable modulus, BC sheets seem to be an ideal candidate as raw material to further enhance the Young's modulus of high-strength composites (Park *et al.*, 2009).

### 1.2.3 Thermal behavior

As shown in Figure 8, a BC dry membrane can be heated up to 325°C before it starts to burn, which is at least 75°C above the burning temperature of conventional office paper. This higher thermal resistance can attributed to the absence of additives in its composition, which are common in papermaking. Not only by its thermal, but also by its mechanical properties (tensile strength of 200-300 MPa), BC

could also be an alternative material for industrial seals and connections (Pecoraro *et al.*, 2008).

**Table 4** Mechanical properties of BC and other organic layer material

Material	Young's modulus (GPa)	Tensile strength (MPa)	Elongation (%)
BC	15-35	200-300	1.5-2.0
Polypropylene	1.0-1.5	30-40	100-600
Polyethylene terephthalate	3-4	50-70	50-300
celluphane	2-3	20-100	15-40

**Source:** Park *et al.* (2009).

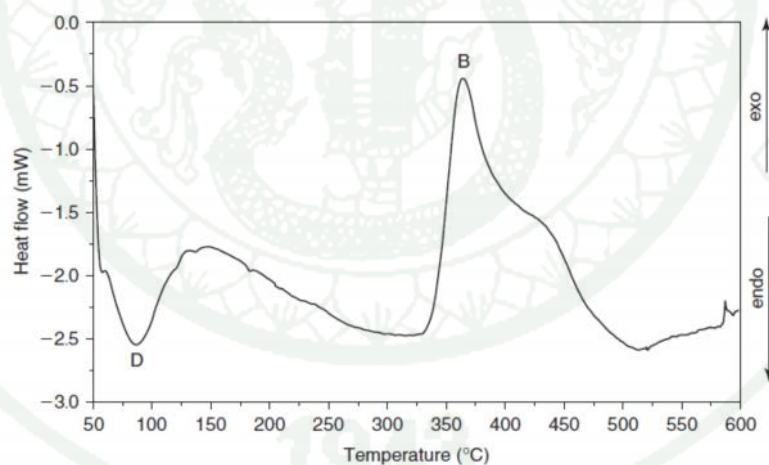


**Figure 8** DSC thermogram of a BC membrane. The temperatures at D and B refer to the dehydration (87°C) and burning (363°C) peak temperatures, respectively.

**Source:** Pecoraro *et al.* (2008)

The specific properties of BC make it interesting for important applications, such as a nutritional component (additive of low caloric contents, stabilizer, texture modifier, *nata de coco*), a pharmacological agent (temporary dressing, excipient, cosmetics, drug carriers), as well as in telecommunications and papermaking, as summarized in Table 5 (Pecoraro *et al.*, 2008).

**Table 5** Examples of applications of BC.

Area	Applications
Cosmetic	Stabilizer of emulsions; component of artificial nails
Textile industry	Artificial textiles; highly absorbent material
Sports and tourism	Sporting clothes; tents; camping material
Mining and refinery	Sponges for recovery spilled oil; material for toxin adsorption
Wastes treatment	Recycling of minerals and oils
Sewage purification	Urban sewage purification; water ultrafiltration
Broadcasting	Sensitive diaphragms for microphone and stereo headphones
Forestry	Artificial wood replacer, multi-layer plywood, heavy-duty containers
Paper industry	Specialty paper, archival document repairing, more durable banknote, diaper, napkins
Machine industry	Car bodies, airplane part, sealing of cracking in rocket casings
Food production	Edible cellulose ( <i>nata de coco</i> )
Medicine	Temporary artificial skin for therapy of burns and ulcers, component of dental implants
Laboratory	Immobilization of protein, cells; chromatographic techniques; medium for tissue cultures
New application	Cellulose thin films for document and book recovery; fibres (including optical); luminescent material; fuel cell membranes; drug delivery; stents covering; ophthalmic, cardiovascular and neurological prostheses.

**Source:** Pecoraro *et al.* (2008)



### 1.3 BC for composites application

Composite materials are engineered materials made from two or more constituents with significantly different mechanical properties, which remain separate and distinct within the finished structure. There are two categories of constituent materials: matrix (matrix phase) and reinforcement (dispersed phase). Matrix phase is the primary phase having a continuous character. Matrix is usually more ductile and less hard phase. It holds the dispersed phase and shares a load with it. Dispersed (reinforcing) phase is embedded in the matrix in a discontinuous form. This secondary phase is called the dispersed phase. Dispersed phase is usually stronger than the matrix, therefore, it is sometimes called reinforcing phase (Jose *et al.*, 2012). Based on the matrix material which forms the continuous phase, the composites are broadly classified into polymer matrix composites (PMC), metal matrix (MMC) and ceramic matrix (CMC). Of these, polymer matrix composites are much easier to fabricate than MMC and CMC. This is due to the relatively low processing temperature required for fabricating polymer matrix composite (Mathew, 2009). Fiber reinforced composites contain reinforcements having lengths higher than cross sectional dimension. Fibrous reinforcement represents physical rather than a chemical means of changing a material to suit various engineering applications (Mathew, 2009). These can be broadly classified as shown in figure 9

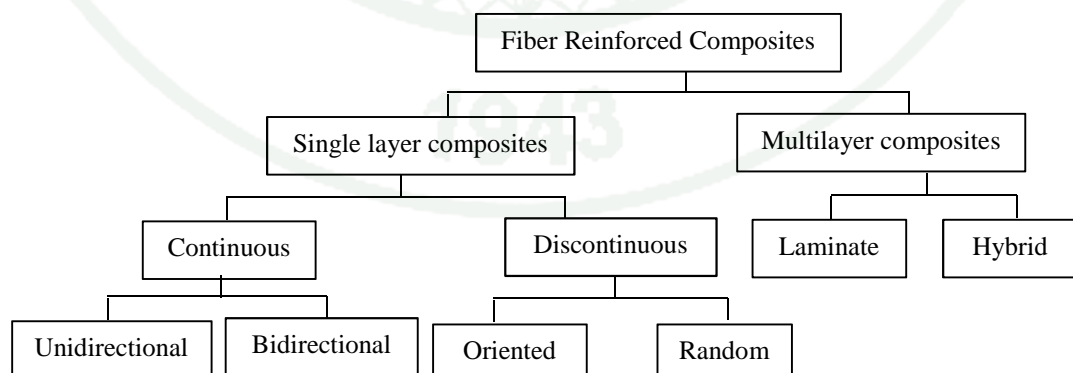


**Figure 9** Classification of fiber reinforced composites.

**Source:** Mathew (2009)

Reinforcing fiber in a single layer composite may be short or long based on its overall dimensions. Composites with long fibers are called continuous fiber reinforcement and composite in which short or staple fibers are embedded in the matrix are termed as discontinuous fiber reinforcement (short fiber composites). In continuous fiber composites fibers are oriented in one direction to produce enhanced strength properties. In short fiber composites, the length of short fiber is neither too high to allow individual fibers to entangle with each other nor too small for the fibers to lose their fibrous nature. The reinforcement is uniform in the case of composites containing well dispersed short fibers. There is a clear distinction between the behavior of short and long fiber composites (Mathew, 2009). Therefore, some researchers have done investigations on BC reinforced polymer composites.

Gindl and Keckes (2004) reported that composites of cellulose acetate butyrate reinforced with cellulose sheet synthesized by *Glucanacetobacter xylinum* were produced by solvent evaporation casting. The composites contained 10% and 32% volume cellulose, and showed a Young's modulus of 3.2 and 5.8 GPa, and a strength of 52.6 and 128.9 MPa, respectively, in tensile tests. Stress-strain curves showed bi-phasic material characteristics, with an initial linear behaviour, followed by yielding, and a second linear phase until fracture.

Gabr *et al.* (2010) investigation concerned the manufacturing of a new type of composite with the goal of studying. Effect of adding BC (BC) as natural fiber to plain woven carbon fiber reinforced plastic (CF)/epoxy modified with liquid rubber (Carboxyl-Terminated Liquid Butadiene-Acrylonitrile – CTBN) on the mechanical properties and thermal properties has been investigated. Addition of 0.5% of BC to composite modified with 10% liquid rubber improved the storage modulus by 28% at 200 °C indicating that the combination of BC and CTBN contribute to improve the heat resistance of the composite.

Barud *et al.* (2011) investigated BC (BC)/poly(3-hydroxybutyrate) (PHB) composite membranes. There were prepared from chloroform-swollen BC membranes and PHB chloroform solutions. Relative contents were varied from 25 to 90 (% w/w)

of PHB. Improved mechanical properties were observed for the composites compared to the individual components suggesting potential applications for the new biodegradable materials.

Wan *et al.* (2009) studied BC nanofibres which were used as the biodegradable reinforcement. The BC/starch biocomposites possess much higher tensile strength and modulus than the unreinforced starch, but show lower elongation at break. The tensile strength of the BC/starch biocomposite containing 15.1 wt.% BC nanofibres and the starch decreases drastically upon exposure to microorganism attacks. The BC/starch biocomposite shows higher retention when compared to the starch owing to the higher resistance to microorganism attacks of the BC fibres in comparison to starch.

Martins *et al.* (2009) reported that BC was used as reinforcement in composite materials with a starch thermoplastic matrix. All composites showed good dispersion of the fibers and a strong adhesion between the fibers and the matrix. The composites prepared with BC displayed better mechanical properties than those with vegetable cellulose fibers. The Young modulus increased by 30 and 17 fold (with 5% fibers), while the elongation at break was reduced from 144% to 24% and 48% with increasing fiber content, respectively for composites with bacterial and vegetable cellulose. These materials are promising candidates in applications like food packaging and biodegradable artifacts.

#### 1.4 BC for nanocomposites application

Nanocomposites are topical, and literature on nanocellulose or cellulose nanoparticle is becoming abundant in recent years (Siqueira *et al.*, 2010b). The concept of nanostructured material design is gaining widespread importance among the scientific community because of their biodegradability (John and Thomas, 2008), strength and other characteristic (Siqueira *et al.*, 2010a). Nanocomposites describe a class of two-phase material where one of the phases has least one dimension lower than 100 nm (Bendahou *et al.*, 2009). Nanocomposites use matrixes where the

nanosizes reinforce elements are dispersed (Siqueira *et al.*, 2010b). The outstanding reinforcement of nanocomposite is primarily attributed to the large interfacial area per unit volume or weight of the dispersed phase. The nanolayers have much higher aspect ratio than typical microscopic aggregates. The three major advantages that nanocomposites have over conventional composites are as follows (Mathew, 2009).

- I. Lighter weight due to low filler loading
- II. Low cost due to fewer amount of filler use
- III. Improved properties such as mechanical, thermal, optical, electrical, barrier etc., compared with conventional composites at very low loading of filler.

According to George *et al.* (2011) studied nanocrystals which prepared from BC are considered as 'green nanomaterials'. Using this enzyme processed BC nanocrystals (BCNC), Polyvinylalcohol (PVA) nanocomposite films were prepared and characterized. Incorporation of these nanocrystals in polymer matrix resulted in a remarkable improvement in the thermal stability as well as mechanical properties of nanocomposite films. These nanocomposites exhibited higher melting temperature ( $T_m$ ) and enthalpy of melting ( $\Delta H_m$ ) than those of pure PVA, recommending that the addition of nanocrystals modified the thermal properties of PVA. The effective load transfer from polymer chains to the BCNC resulted in an improved tensile strength from 62.5 MPa to 128 MPa, by the addition of just 4 wt% of BCNC. Furthermore, the elastic modulus was found to increase from 2 GPa to 3.4 GPa. The BCNC obtained through cellulose treatment under controlled conditions were associated with several desirable properties and appear to be superior over the conventional methods of nanocrystals production.

Hu *et al.* (2009) studied BC nanofiber-reinforced unsaturated polyester resin composites (BC/UP). The results show that coupling treatment did not change the morphology of BC nanofibers, while it changed the chemical states of the BC fiber's surface. The X-ray photoelectron spectroscopy (XPS) result indicated that chemical bonding was formed at the interface between unsaturated polyester resin



(UPR) matrix and BC fibers after surface treatment. The mechanical property results showed that after BC modification, tensile strength, flexural strength, shear strength and Young's modulus of the BC/UPR composites were increased by 117.7%, 38.4%, 38.7% and 27.6% respectively.

Grande *et al.* (2009) studied BC-starch self-assembled nanocomposites. Potato and corn starch were added into the culture medium and partially gelatinized in order to allow the cellulose nanofibrils to grow in the presence of a starch phase. Structural properties determined by XRD and ATR-FTIR showed that the crystallinity of BC was preserved in spite of the presence of starch, hence the mechanical properties of the nanocomposites showed no significant decrease.

Woehl *et al.* (2010) studied BC that was used as reinforcement agent in glycerol-plasticized cassava starch bionanocomposites before and after treatment with *Trichoderma reesei endoglucanases*. The elastic modulus of the bionanocomposite ( $575.7 \pm 166.7$  MPa) was 17 times higher than that of the starch matrix ( $33.4 \pm 4.3$  MPa) and four times higher than that of the film containing untreated fibres ( $140.6 \pm 40.3$  MPa). Similarly, the tensile strength ( $8.45 \pm 2.35$  MPa) was increased by a factor of eight in relation to the former ( $1.09 \pm 0.39$  MPa) and almost doubled in relation to the latter ( $4.15 \pm 0.66$  MPa). Hence, BC nanofibres were shown to be excellent reinforcement agents for the production of starch-based bionanocomposites.

## 2. Cellulose nanowhiskers

Cellulose is the main building material out of which woods are made, there are other major sources such as plant fibers (cotton, hemp, flax, etc.), marine animals (tunicate), or algae, fungi, invertebrates, and bacteria (Lavoine *et al.*, 2012). Natural fibers mainly consist of cellulose, lignin, and hemicellulose but also include low quantities of pectin, pigments and extracts. Cellulose chains are bio-synthesized by enzymes, deposited in a continuous fashion and aggregated to form microfibrils. The microfibrils further aggregate on the macroscale to form fibers (Chen *et al.*, 2012).

Cellulose is a natural polymer consisting of D-anhydroglucose ( $C_6H_{11}O_5$ ) repeating units joined by 1,4-  $\beta$ -D-glycosidic linkages at C1 and C4 position. The degree of polymerization (DP) is around 10,000 (John and Thomas, 2008). Each repeating unit contains three hydroxyl groups at C-2, C-3 and C-6 linkages (Fig. 10) (John and Thomas, 2010). C-6 is a primary hydroxyl, which is the most reactive position for esterification reactions while C-2 is the more acidic of the two secondary hydroxyl groups and is the more reactive site for etherification (Gardner *et al.*, 2008). The three hydroxyl groups and their ability to hydrogen bond play a major role in directing the crystalline packing and also govern the physical properties of cellulose (John and Thomas, 2008). Cellulose is very stable in a variety of solvents and can only be dissolved by the application of strong acids or strong hydrogen bonding solvent systems, usually amine-based. The thermal properties of cellulose are such that the cellulose glass transition temperature is in the range of 200 to 230 C, which is close to its thermal decomposition temperature of 260 C (Gardner *et al.*, 2008).

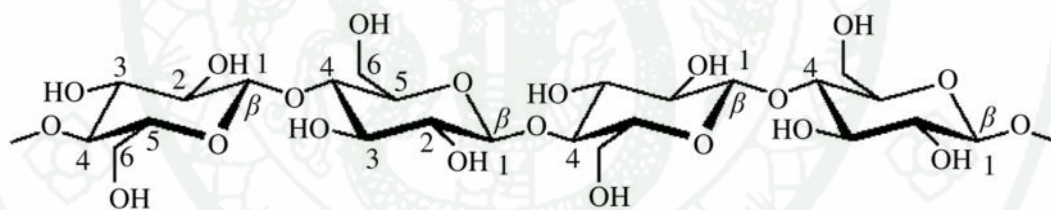


**Figure 10** Position of hydroxyl groups on cellulose backbone

**Source:** Gardner *et al.* (2008)

Cellulose nanowhiskers, the generally accepted and overused trade name of cellulosic nanoparticles, include cellulose nanocrystals or whiskers, and cellulose microfibrils or microfibrillated cellulose (MFC). The former are obtained by submitting natural fibers to strong acid hydrolysis followed by a sonication treatment to obtain stiff rod-like nanoparticles (Belbekhouche *et al.*, 2011). The term cellulose nanowhiskers (CNWs) refer to the needlelike structure of cellulose monocrystals. These crystals are linked by amorphous cellulose and form cellulose microfibrils,

which are the reinforcing phase of the wood cell wall. The cellulose nanowhiskers have attracted great interest as a novel nanostructured material during recent years. These crystallites are expected to be used as reinforcement in polymers and pharmaceutical products such as hydrogels, etc (Oksman et al., 2011).

Recently, nanocellulose has been growing interested for many researches because of its displays unique characteristics, such as very large surface to volume ratio, high surface area, good mechanical properties including high Young's modulus, high tensile strength, high elasticity (Chen *et al.*, 2011; Klemm *et al.*, 2011), and low coefficient of thermal expansion (Kaushik *et al.*, 2010). In case of the morphology of cellulose nanofibers is nano-whisker or rod-like shape. Commonly, diameter and length of nanocellulose present ranging 5-15 nm and 100-300 nm, respectively (Klemm *et al.*, 2005), which depended on extraction methods, chemical agents used, reaction time, temperature (Rosa *et al.*, 2010) as well as cellulose sources. The size, shape, functions, properties of nanocellulose depend mainly on the cellulosic source and preparation methods used (Brinchi *et al.*, 2013). Klemm *et al.* (2011) and Brinchi *et al.* (2013) proposed about the nomenclature of nanocellulose in many types, as indicated in Table 2. At the same time, the applications of nanocellulose have been extending interested for research involves the use of nanocellulose in many fields. For instance of filler or reinforcing agents in many polymers to improve their properties.

## 2.1 Preparation of nanocellulose by acid hydrolysis

Several methods for preparing nanowhiskers have been developed in recent years. These methods include physical treatments, e.g. shearing or high-pressure homogenizing; chemical treatments, e.g. acid hydrolysis; biological treatments, e.g. enzyme-assisted hydrolysis; synthetic and electrospinning methods, as well as a combination of the methods mentioned above (Chen *et al.*, 2009). Among the methods developed to extract nanowhiskers from cellulose, acid hydrolysis is the most well-known and widely used. Nickerson and Habrle (1947) disclosed the use of hydrochloric and sulfuric acid hydrolysis to produce crystallites from cellulose materials, and Ranby (1952) reported the preparation of cellulose whiskers from



microfibrils, also using acid hydrolysis. So that, the acid hydrolysis could be possibly used to obtain the nanocelluloses, and the dimensions of nanocelluloses are basically dependent not only on the acid species, acid concentration, time, and temperature of hydrolysis reaction, but also on the different origins of cellulose.

Acid hydrolysis treatment was two primary steps for isolation of cellulose nanowhiskers by sulfuric acid hydrolysis. The first was the diffusion of sulfuric acid into the cellulose fibers, and subsequently, the cleavage of glycosidic bonds to separate cellulose fibrils. This condition must be maintained to avoid the occurrence of complete hydrolysis to glucose. The second was appropriate use of mechanical treatment (i.e. sonication treatment) to disperse cellulose nanowhiskers in the aqueous phase. Figure 11 shows the proposed reaction of sulfuric acid and the surface hydroxyl groups of cellulose to produce the charged surface sulfate ester which improve dispersion of the cellulose nanowhiskers in water (Fahma *et al.*, 2011).

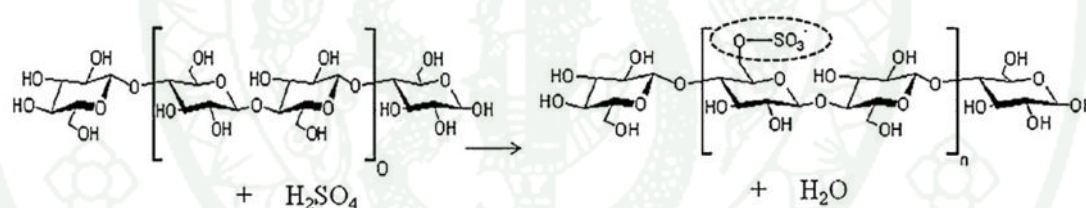


**Figure 11** Forming charged surface sulfate ester group of cellulose nanowhiskers

**Source:** Fahma *et al.* (2011)

The concepts of nanocellulose preparation involves about the difference of cellulose structure. It is well known that cellulose structure has two major regions (Figure 12). One is crystalline regions (some authors called ordered structure) and another is amorphous regions. Resulting from those regions has different properties such as thermal properties and digestibility. Thus, the amorphous regions can be destroyed by different treatments before crystalline region because of the treatment process starts with the cleavage and destruction of the more readily accessible amorphous regions to liberate rod-like crystalline cellulose sections. Therefore,

several researches have been studied attempt to eliminate amorphous region using different techniques in order to generate crystalline nanocellulose fibers. After remove the amorphous region, the residue crystalline region of cellulose chain exhibited the rod-like shape in nano-dimensional structure, depending on source and methods used, which present the potential properties such as high crystallinity, good mechanical properties, high aspect ratio when compare with native cellulose.

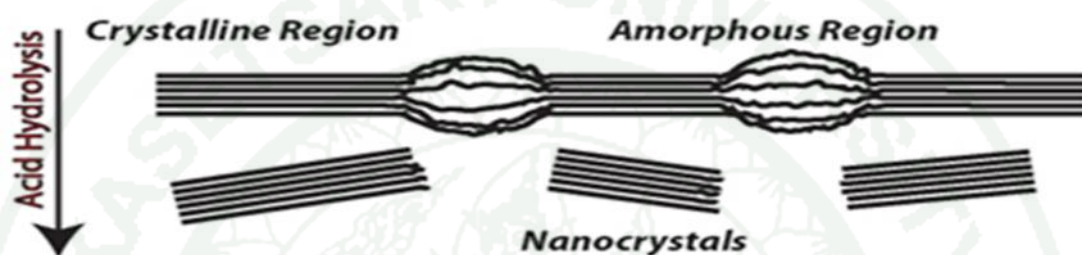


**Figure 12** Acid hydrolysis breaks down disordered (amorphous) regions and isolates nanocrystals.

The acid hydrolysis is the most well-known and widely used for the preparation of nanocellulose (Bondeson and Oksman, 2007; Hashaikh and Abushammala, 2011; Chen *et al.*, 2012). For example of chemical agents were using for acid hydrolysis, such as sulfuric acid (Mandal and Chakrabarty, 2011), hydrochloric acid (Kaushik and Singh., 2011), oxalic acid (Cherian *et al.*, 2008; Deepa *et al.*, 2011) as well as acid mixture (Corrêa *et al.*, 2010). Generally, acid hydrolysis was carried out with sulfuric acid with constant stirring. The amorphous regions around the cellulose microfibrils could be destroyed by acid hydrolysis under controlled conditions, keeping the crystallites intact. The acid hydrolysis is selective in cellulose fibrils, resulting in colloid suspensions of cellulose nanofibers (Alemdar and Sain, 2008b). Nanocellulose obtained by acid hydrolysis of cellulose chain (microfiber) has a wide range in size, depending on sources and process used. Treating the cellulose fibers (lignin and hemicellulose free) with sulfuric acid involves esterification of hydroxyl groups, besides the hydrolysis of the glycosidic linkages rendering extensive reduction in degree of polymerization (DP) and particle size consequently (Mandal and Chakrabarty, 2011).

### 3. Natural rubber

Natural rubber is obtained by tapping the tree *Hevea brasiliensis*. It consists of 30-35% rubber, 60% aqueous serum, and 5-10% other constituents such as fatty acid, amino acid and proteins, starch, sterols, esters and salt. Natural rubber is the prototype of all elastomers. It consists primarily of isoprene. Regarding to 95% of isoprene production is used to produce *cis*-1,4-polyisoprene (Figure 13). Molecular weight of natural rubber was ranging from 1 to  $2.5 \times 10^6$ . Some natural rubber sources called gutta percha are composed of *trans*-1,4-polyisoprene, a structural isomer which has similar, but not identical properties. However, because of the double bonds in NR chain, result in its sensitivity to heat and oxidation. Therefore, NR is vulcanized with sulfur compounds, which can crosslink the chain because of the presence of the reactive double bonds. It has strain induced crystallization at low temperature that be have high strength, hot tear resistance, retention of strength at elevated temperature, excellent dynamic properties and general fatigue resistance, so it has accounted for its use in many applications.

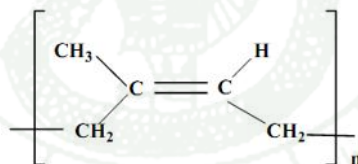


**Figure 13** The structure of *cis*-1,4 polyisoprene

Natural rubber becomes soft at high temperature and brittle at low temperatures. Therefore, vulcanization is a dominant method to improved its properties on reacting with sulphur at high temperature. Sulphur forms cross links at the reactive sites of double bonds and thus the rubber gets stiffened. In the manufacture of tyre rubber, 5% of sulphur is used as a crosslinking agent. The probable structures of vulcanised rubber molecules.

### 3.1 Natural fiber reinforced natural rubber composites

Ismail *et al.* (2002) studied the bamboo fibre reinforced natural rubber composites. It was found that tensile modulus and hardness of composites increased with increasing filler loading and the presence of bonding agents. The adhesion between the bamboo fibre and natural rubber can be enhanced by use of a bonding agent. The scorch time ( $t_2$ ) and cure time ( $t_{90}$ ) decrease with increasing filler loading and the presence of bonding agent.

De *et al.* (2004) studied the effect of grass fiber filler on curing characteristics and mechanical properties of natural rubber. It was found that 400 mesh grass fiber loaded natural rubber composite showed superior mechanical properties. Optimum cure time increased with the increase in fiber loading but the change in scorch time was less. With increase in the fiber loading, modulus and hardness of the composite increased but tensile strength decreased.

Jacob *et al.* (2004) studied effects of concentration and modification of fiber surface in sisal/oil palm hybrid fiber reinforced rubber composites. It was found that addition of sisal and oil palm fibers led to the decrease of tensile strength and tear strength but increased modulus. The extent of adhesion between fiber and rubber matrix was found to increase on alkali treatment of fibers. From the mechanical properties the alkali treated fibers exhibited better tensile properties than untreated composites.

Joseph *et al.* (2010) investigated the dynamic mechanical properties of natural rubber reinforced with macro/micro fibrils of oil palm fiber. They found that addition of macro/microfibers decreased the damping characteristics of composites. It was contain microfibrils treated with silane coupling agent showed maximum dynamic properties. The glass transition shifted to the positive side on the addition of treated microfibers. It was found that the incorporation of treated microfibrils decreased the damping characteristics of the composite as the fibers acted as barriers to the free movement of the macromolecular chain.



Mathew and Joseph (2007) studied the mechanical properties of short isora fiber reinforced NR composites which were enhanced by chemical treatment on the fiber surface and by the use of bonding agent. The optimum length and loading of isora fiber in the NR composites were being 10 mm and 30 phr, respectively, for the achievement of good reinforcement.

Lopattananon *et al.* (2006) investigated the influences of untreated fiber content and orientation on the processing and mechanical properties of the composites. The composite stiffness significantly increased while the tensile strength and elongation at break decreased with increasing of fiber contents.

A survey of the literature has shown that studies on cellulosic nanofiber-reinforced NR have been mostly unexplored. With the exception of studies conducted by research groups in France and recently in India, only a limited amount of work is reported in literature.

Siqueira *et al.* (2010b) studied natural rubber nanocomposite films reinforced with cellulose whiskers extracted from capim dourado (CD) were prepared by film casting. CD whisker reinforced natural rubber nanocomposites showed relatively high modulus and strength properties (compared to some selected cellulosic nanocomposites) but lower elongation at break. A possible explanation could be stronger inter-nanoparticles interactions than for other polysaccharide nanocrystals. The reinforcing effect observed above the glass transition temperature of the matrix was higher than the one observed for other polysaccharide nanocrystals and cellulose whiskers extracted from other sources.

Bras *et al.* (2010) isolated cellulose whiskers from bleached sugar cane bagasse kraft pulp. The length and width of the isolated whiskers was in the range 84–102nm and 4–12 nm, respectively. They were used as reinforcing elements in natural rubber (NR) matrix. The results show that significant improvement of Young's modulus and tensile strength was observed as a result of addition of whiskers to the



rubber matrix especially at high whiskers' loading. Differential scanning calorimetry (DSC) results showed no change in the glass transition temperature ( $T_g$ ) of the rubber matrix upon addition of cellulose whiskers but at softening of rubber, cellulose whiskers have reinforcing effect on the rubber. Presence of cellulose whiskers increased the rate of degradation of rubber in soil.

Bendahou *et al.* (2010) prepared cellulose whiskers and microfibrillated cellulose (MFC). The former occurred as rod-like nanoparticles with an average length and diameter around 260 and 6.1 nm, respectively, whereas MFC occurs as very long flexible entangled and partially defibrillated filaments. These cellulosic nanoparticles were used as reinforcing phase to prepare nanocomposite films by the casting/evaporation using latex of natural rubber as matrix. All the results showed that higher filler-matrix adhesion dominated the behavior of MFC-based composites. It resulted in lower water uptake and higher mechanical properties in terms of stiffness. However, the ductility of MFC-reinforced materials is much lower compared to whiskers-based nanocomposite films resulting in a lower shrinkage for the latter during successive tensile tests. The higher MFC–NR interactions resulted in the clear splitting of the main relaxation peak associated with  $T_g$  of the NR matrix. It was supposed to be induced by the formation of an interfacial layer surrounding the filler and which mobility is restricted compared to the bulk matrix.

1943

## MATERIALS AND METHODS

### Materials

#### 1. Raw Materials

- 1.1 Natural Rubber (NR), Block rubber STR5L (Standard Thai Rubber), Thailand
- 1.2 Latex, Dry Rubber Content 60%, Thai Rubber latex group, Thailand

#### 2. Microorganism

- 2.1 *Acetobacter xylinum* AGR 60 was pur The Institute of Food Research and Product Development, Kasetsart University, Bangkok, Thailand

#### 3. Chemical

- 3.1 NaOH, Mallinckrodt Baker, Inc, Malaysia
- 3.2 Sulfuric acid ( $H_2SO_4$ ), RCI labscan Limited, Thailand
- 3.3 ZnO, an activator, Global Chemistry, Thailand.
- 3.4 Stearic acid, an activator, Imperial Industrial, Thailand.
- 3.5 Sulfur, crosslinking agent, Sahapaisai Industry, Thailand.
- 3.6 N-tert-butyl-2-benzothiazole sulfenamide (TBBS), an accelerator, Flexsys, Germany
- 3.7 Sucrose, Mitrophol, Thailand
- 3.8 Acetic acid,
- 3.9 Ammonium sulfate,

#### 4. Equipments

- 4.1 Incubator, Memmert, Germany
- 4.2 Hot plate stirrer, IKA, Germany

- 4.3 Overhead stirrer, IKA, Germany
- 4.4 Water bath, Memmert, Germany
- 4.5 Balance, Mettler Toledo, Switzerland
- 4.6 Centrifuge, Sorval Model RC, Germany
- 4.7 Dialysis membranes, CelluSeq, USA
- 4.8 Sonicator bath, Branson Model 2210R-MT, USA
- 4.9 Two Roll Mill 8×12 inch., model LRM 150, Labtech, Korea
- 4.10 Moving Die Rheometer (MDR), Tech PRO Model 11T202, USA
- 4.11 Hardness, Cogenix, Wallace
- 4.12 Tensile, Shimadzu model AGS-J testing machine, Japan
- 4.13 Tear strength, Instron Universal Testing Machine Model 5569, USA
- 4.14 Fourier transformed infrared spectrometer (FTIR spectrometer), Bruker  
Tensor 27 spectrometer, USA
- 4.15 X-ray diffraction (XRD), Philips Model X'Pert Powde, Japan
- 4.16 Transmission electron microscopy (TEM), JEOL Model JEM 1220,  
Japan
- 4.17 Scanning Electron Microscopy, JEOL Model JSM-5600 LV, Japan
- 4.18 Differential Scanning Calorimeter, Mettler Toledo, Model DSC1,  
Switzerland
- 4.19 Thermogravimetric Analysis, Mettler Toledo, Model TGA/DSC1,  
Switzerland
- 4.20 Dynamic Mechanical Analyser (DMA), model Eplexor 25N, GABO,  
Germany
- 4.21 Atomic force microscopy (AFM), Asylum Model MFD-3D AFM(bio),  
USA

## Methods

### 1. Preparation of BC

The medium for the inoculums was coconut water containing 5.0% sucrose, 0.5% ammonium sulfate and 1.0% acetic acid. The medium were sterilized at 121 °C for 30 min. The inoculum medium was prepared by transferring 50 ml of stock culture to 1000 ml of medium. After the surface pellicle was removed, 5% (v/v) of inoculum was added to the main culture medium. The 1000 ml of activated culture medium was inoculated in a plastic box which covered by filter cloth and incubated statically at room temperature for 7 days. BC pellicles were collected and washed with running tap water and then immersed in 1% NaOH for 2 days at room temperature to remove bacterial cells in the pellicle and rinsed with tap water until the pH was 7. BC pellicles were pressed with hydraulic press to remove water surplus in the pellicle. The BC sheets were dried in a hot air oven at 50 °C for 7 h. Afterward, the BC sheets was grinded with roter mill and then sieved to less than 178 µm (80 mesh). The BC powder was stored in plastic bag and kept in desiccator before use. BC powders were used as reinforcing agent in natural rubber and to prepare BC nanowhiskers by acid hydrolysis.

### 2. Preparation of BCNWs

BC powders were dispersed in 100 ml of 64 %wt sulfuric acid solution under mechanical stirring. Hydrolysis was performed at 60 °C under vigorous stirring for 40 min. The suspension was diluted with cold distilled water to stop the reaction, which was partially neutralized with 40 wt% sodium hydroxide aqueous solution. The diluted suspension was centrifuged at 13,000 rpm for 15 min to obtain the precipitates. The precipitate was suspended with cold distilled water again with strong agitation, followed by a centrifugation. The mixture was washed by successive centrifugations with deionized water until neutrality was achieved. It was dialysed against distilled water for 3 days. The neutral suspension was ultrasonicated for 5 min and stored in a refrigerator. BCNWs have been characterized and were used as

reinforcing phase to prepare nanocomposites films using latex of natural rubber as matrix.

### 3. Preparation of BC/NR composites

The utilization of BC powders as reinforcing filler for NR composites was studied. BC/NR composites were prepared with a laboratory two-roll mill. The cure characteristics, mechanical properties, thermal properties and tensile fracture surface are investigated.

**Table 6** Formulation of the NR/BC Composites

Ingredients	Mixes (phr <sup>a</sup> )				
	C	BC5	BC10	BC15	BC20
Natural rubber	100	100	100	100	100
Bacterial cellulose powder (filler)	-	5	10	15	20
Zinc oxide (activator)	5	5	5	5	5
Stearic acid (activator)	2	2	2	2	2
TBBS <sup>b</sup> (accelerator)	0.7	0.7	0.7	0.7	0.7
Sulfur (vulcanizing agent)	2.25	2.25	2.25	2.25	2.25

<sup>a</sup> Parts per hundred of rubber, <sup>b</sup> *N-tert*-Butyl-2-benzothiazyl sulphenamide.

Mixing formulation showed in Table 6. The composite materials were in a laboratory two-roll mill at 70 °C for 10-15 minutes. The natural rubber was first masticated for 2 min to form a band, followed by the sequential addition of the additives in the order BC powder, ZnO, stearic acid, TBBS (accelerator), and sulfur. After homogenization they were sheeted out and kept at room temperature for 24 hours before testing. Prior to vulcanize the mixes, a vulcanization time was determined by means of Moving Die Rheometer (MDR). The degree of vulcanization determines the cure characteristic of the sample as it is heated and compressed. The test is known as a cure curve such as scorch time, time to percentage cure, maximum and minimum torque. The mixes were compression molded using a hydraulic hot



press at 150 °C, under pressure 15 MPa with the optimum cure time ( $t_{c90}$ ) corresponding to the rheometer test.

#### **4. Preparation of BCNWs/NR nanocomposites**

BCNWs were used as reinforcing phase to prepare nanocomposites films using latex of natural rubber as matrix. There were obtained by casting method, and effects of BCNWs on mechanical properties, thermal properties and tensile fracture surface were investigated.

The suspension of BCNWs and NR latex were mixed in various proportions in order to obtain final dry composites films ranging between 2 and 2.3 mm in thickness and with 0-15% weight fraction of solid BCNWs in NR matrix. The mixture was stirred using an overhead stirrer for 8 h to obtain a uniform dispersion of BCNWs in NR latex. Films were cast in Teflon molds. The films were dried in a ventilated oven at 40°C for several days depending on the amount of filler (and water) in the mixture.

#### **5. Physical characterizations**

##### **5.1 Scanning electron microscopy**

Surface morphology of tensile fracture surfaces of the composites was carried out using a scanning electron microscopy (SEM) model Jeol JSM-5600 LV. In order to avoid from electrostatic changing, the specimens were sputter coated with gold prior process.

##### **5.2 Transmission electron microscopy (TEM)**

Transmission electron micrographs of BCNWs were taken with a JEOL Model JEM 1220 with an acceleration voltage of 80 kV. BCNWs were deposited from an aqueous dispersion on a microgrid (200 mesh) cover with thin carbon film. The samples were stained with a 1% (w/w) uranyl acetate (UA) solution.

### 5.3 X-ray diffraction (XRD)

The x-ray diffraction patterns were measured for both BC and BCNWs with x-ray diffractometer (Philips model X'Pert Powder). The configuration of the equipment was  $-2^\circ$  and the samples were examined over the angular range of  $5^\circ$  to  $45^\circ$  with a step size of 0.02 and a count time of 4s per point. The crystallinity index (CI%) was estimated on the basis of areas under crystalline and amorphous peaks after an appropriate baseline correction and the applying of a deconvolution technique.

$$\text{Crystallinity index (\%CI)} = \frac{\text{Crystalline area}}{(\text{crystalline area} + \text{amorphous area})} \times 100$$

### 5.4 Fourier transform infrared spectroscopy (FTIR)

The BC and BCNWs mixed with potassium bromide (KBr) powder were pressed into a small pellet and FTIR spectra were recorded on Nicolet model 5700 in the absorption mode with a resolution of  $4 \text{ cm}^{-1}$  in range of  $4000\text{-}400 \text{ cm}^{-1}$ .

## 6. Thermal characterizations

### 6.1 Thermo gravimetrical analysis (TGA)

TGA was performed with a Mettler Toledo model TGA/DSC1 for BC powder, BCNWs, NR and BCNWs/NR nanocomposites. The sample (2-5 mg) was heated from 50 to  $600^\circ\text{C}$  with a heating rate of  $10^\circ\text{C}/\text{min}$  under nitrogen atmosphere.

### 6.2 Differential Scanning Calorimeter (DSC)

Glass transition temperature of the NR, BC/NR composites and BCNWs/NR nanocomposites were determined using DSC (modal DSC 7 Perkin Elmer) inter-lined to the heating module. The instrument was calibrated using Indium standard. Samples weighing 4-5 mg were sealed in aluminium DSC pans using

encapsulating press. The heating rate was 10 °C/min from -85 °C to 200 °C. An empty aluminium pan was used as a reference. Nitrogen gas was purged to the unit to maintain an inert atmosphere.

## **7. Mechanical characterizations**

### **7.1 Tensile Properties**

The dumbbell-shape samples were cut from vulcanized rubber composites and rubber nanocomposites films by a tensile specimen cutter according to ISO 37. The tensile tests were performed using a Shimadzu model AGS-J testing machine (Shimadzu, Japan) with a 1kN load cell. Measurements were carried out with crosshead speed of 500 mm/min at 25°C. The results were obtained on the average of 5 measurements for each composite.

### **7.2 Tear Strength**

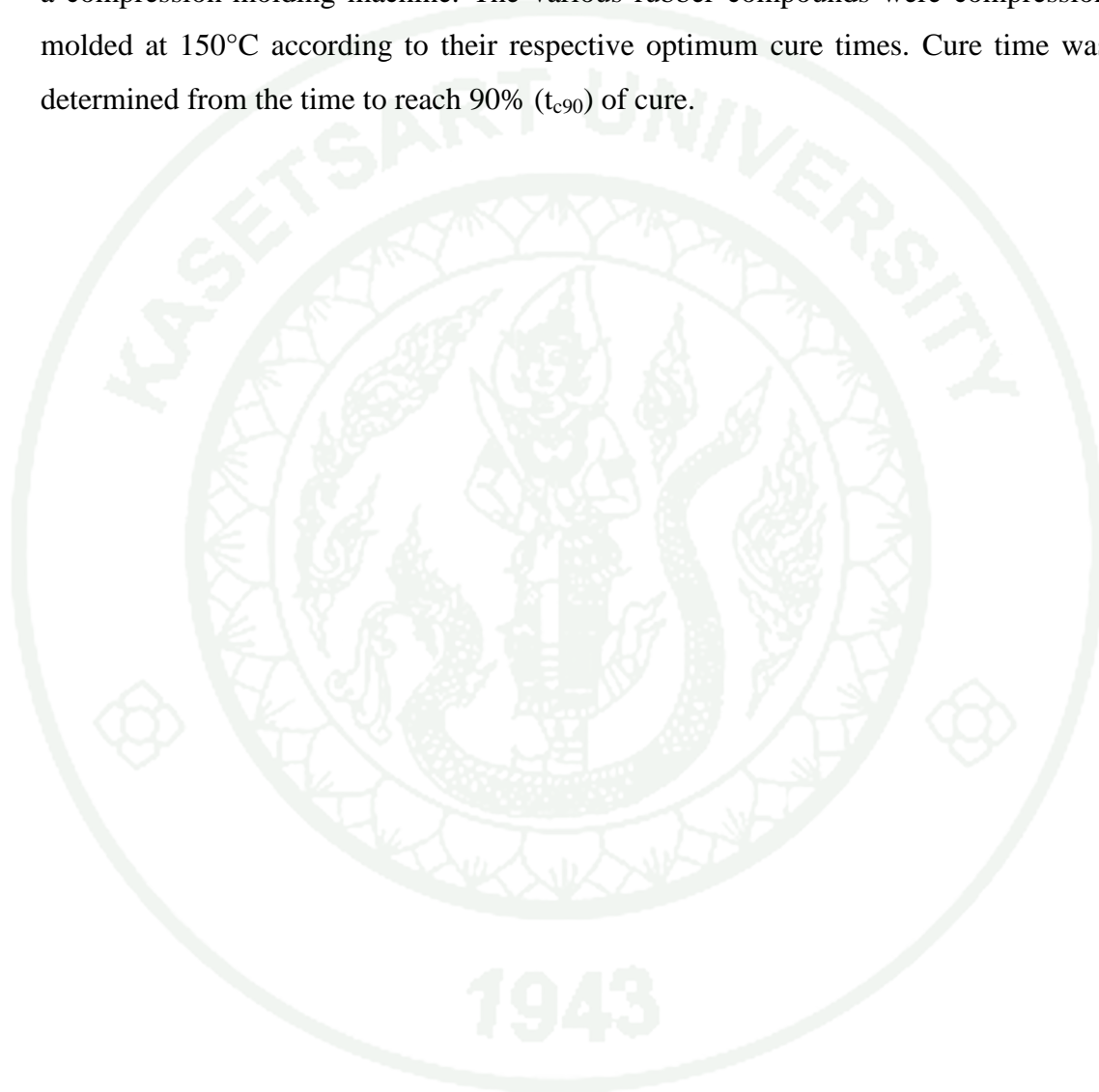
The BC/NR composites were cut into tear specimens (angle shape) by using the punching machine. Testing was carried out on universal testing machine in accordance with ASTM D624-98.

### **7.3 Hardness**

Shore A hardness of BC/NR composites was measured according to ASTM D 2240 using hardness tester. The specimens about 6 mm in thickness were placed on test platform. The durometer was held in a vertical position with point of the indenter at least 12 mm from any edge of the specimens. Five measurements were taken as the hardness value of the test sample.

## 8. Cure Characterisation

The cure characteristics of BC/NR compound having sulfur as curing agent were assessed by Moving Die Rheometer (MDR). Vulcanization was performed using a compression-molding machine. The various rubber compounds were compression molded at 150°C according to their respective optimum cure times. Cure time was determined from the time to reach 90% ( $t_{c90}$ ) of cure.



## RESULTS AND DISCUSSION

### Preparation of BC and BCNWs

BC was produced by *Glucanacetobacter xylinus* in static culture medium (Figure 14a). BC was initially milled in a roller mill machine to pass through a 80 mesh screen. It is observed that more than 80% of the 100 g sample passed through sieve 178  $\mu\text{m}$ . This is shown that more of the particles have sizes less than 178  $\mu\text{m}$  (figure 14b). The BC powders were used to extract BCNWs. BCNWs were obtained by sulfuric acid digestion of bacterial cellulose (BC). The BC powder and BCNWs have been characterized by transmission electron microscopy (TEM), atomic force microscopy (AFM), X-ray diffraction, Fourier transform infrared (FT-IR) spectroscopy and thermal properties.



**Figure 14** Image of (a) BC and (b) BC powder.

### 1. Morphological characterization of BCNWs

In this study, TEM and AFM were used to investigate the morphology and size of the dispersed structures. The morphology of BCNWs suspensions was studied by means of TEM and the cross-sections and lengths of each sample were estimated from several measurements on TEM micrographs. The TEM image of BCNWs prepared by the acid hydrolysis of the BC are shown in figure 15. The analysis of



TEM revealed that BCNWs have diameter ( $d$ ) of  $7 \pm 3.68$  nm and length ( $L$ ) of  $186 \pm 78.1$  nm, giving an aspect ratio ( $L/D$ ) of 28. The aspect ratio of the BCNWs is an important parameter which conditions the reinforcing effect of the nanowhiskers when incorporated into a polymeric matrix. Materials with aspect ratios higher than 30, such as tunicin whiskers ( $L/D \sim 67$ ) have been reported to provide a considerably higher reinforcement effect as compared to nanofillers having lower aspect ratios, such as Avicel whiskers ( $L/D \sim 10$ ) (Azizi Samir *et al.*, 2005). Besides, The diameters measured were similar to the nano-sized structures derived from other sources of agro-residues such as nanofibrils from cassava bagasse (2-11 nm) (Teixeira *et al.*, 2009), sugarcane bagasse (4 nm) (Teixeira *et al.*, 2011), wheat straw (10-80) (Alemdar and Sain, 2008a) and cotton cellulose (10 nm) (Lu and Hsieh, 2010).

AFM was used to investigate the morphology, size and shape because of AFM technique was used to observe in nano-scale (Teixeira *et al.*, 2009). AFM images also presented needle-like nanoparticles (Flauzino Neto *et al.*, 2013). AFM height images collected under tapping mode displayed typical shape of BCNWs (Figure 16) revealed as nano-dimension approximately 5 nm and exhibited numerous and overlapped fibers. The determination of the average diameter of the nanoparticles gives a similar value to the one determined from TEM observation.

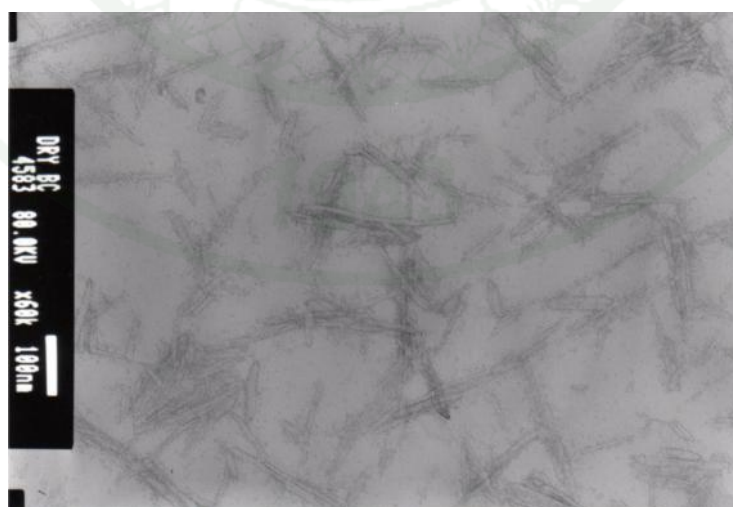


**Figure 15** TEM micrograph of nanowhiskers (BCNWs).

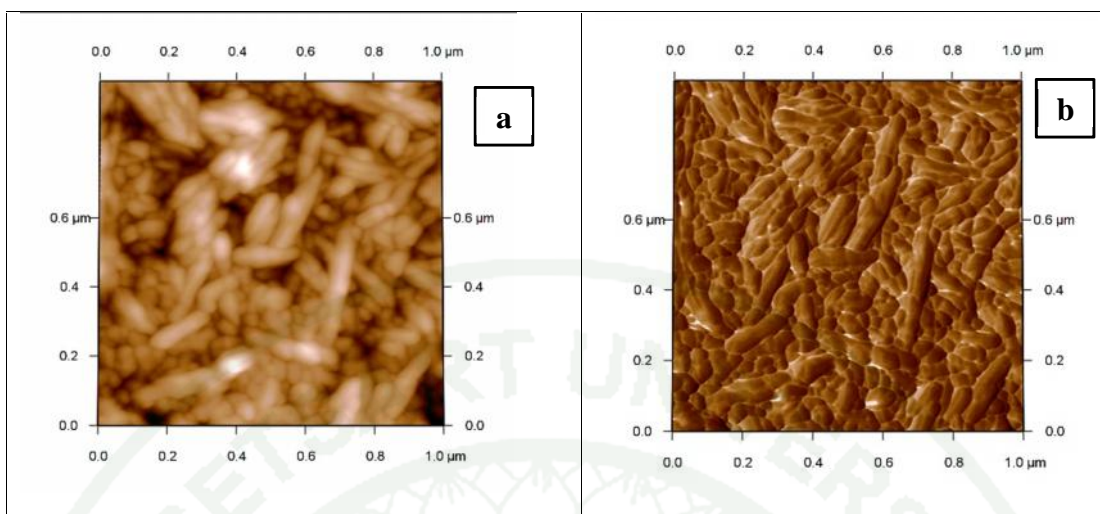


**Figure 16** AFM images of bacterial cellulose nanocrystals obtained after acid hydrolysis treatment (a) height image and (b) phase image.

## 2. X-ray diffraction of BC and BCNWs

Sulfuric acid treatment of cellulosic materials has been widely used as a way to extract nanocrystals since it causes a preferential hydrolysis of disordered or amorphous regions of the material through a surface reaction process, whereas crystalline domains have a higher resistance to acid attack and remain intact under controlled conditions (Martinez-Sanz *et al.*, 2011). X-ray diffraction patterns of BC powder and BCNWs are shown in figure 17. These patterns are typical of semicrystalline material with an amorphous broad hump and crystalline peak (Fahma *et al.*, 2011). Generally, XRD pattern of BC exhibited three reflection peak at  $14.5^\circ$ ,  $16.7^\circ$  and  $22.5^\circ$  were attributed to the BC cultured in static circumstance (Phisalaphong *et al.*, 2008). These diffraction peak are ascribed to cellulose I allomorph (Martinez-Sanz *et al.*, 2011). The crystallinity index (CrI) calculated for the BC powder was 48.73 %. After, acid hydrolysis the CrI of BCNWs increases up to 55.81 %. The increase of 14.53% in the crystallinity index of the BCNWs is similar to the increase of 11.25%. Martinez-Sanz *et al.* (2011) reported for hydrolysis time 48 h. The CrI of BCNWs was higher than BC which can be describe to the removal of

cellulose amorphous domain after acid hydrolysis (Siqueira *et al.*, 2010b; Siqueira *et al.*, 2010a; Siqueira *et al.*, 2010c).

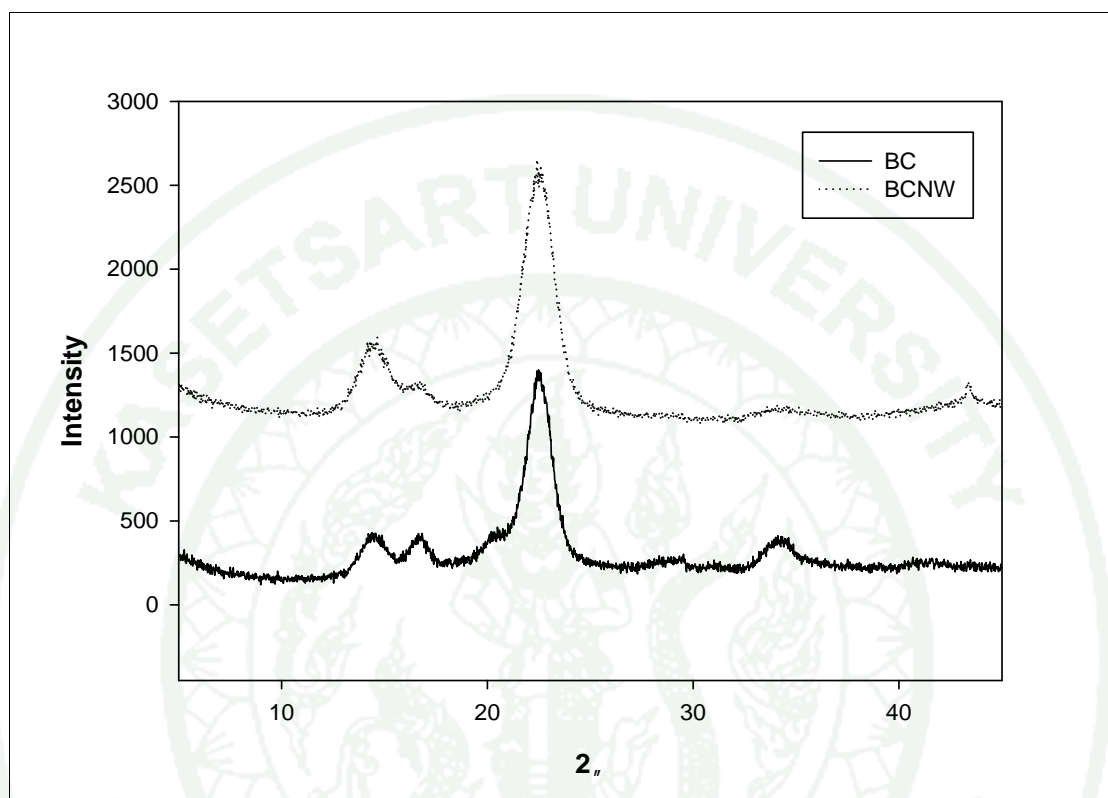


**Figure 17** X-ray diffraction pattern of native bacterial cellulose (BC) and nanowhiskers (BCNW).

### 3. Fourier transformed infrared spectrometer of BC and BCNWs

The FTIR spectra were carried out to characterise the chemical structure by identifying the functional groups present in BC powder and BCNWs. The FTIR spectra of the BC powder and BCNWs are illustrated in figure 16. It was found that no significant differences were observed both native BC and BCNWs. The results show that the cellulose molecular structure remains unchanged following acid hydrolysis. According to the literature (Oh *et al.*, 2011), the bands at  $4000\text{--}2995\text{cm}^{-1}$ ,  $2900\text{cm}^{-1}$ ,  $1430\text{cm}^{-1}$ ,  $1375\text{cm}^{-1}$  and  $900\text{cm}^{-1}$  are known to be especially sensitive to the cellulose molecular order. Broadening of these bands is related to greater disorder

in the polysaccharide phase morphology and thus, the shape of these bands can be related to the amount of crystalline vs. amorphous fractions in cellulose. Even though the crystallinity index estimated by means of XRD is not significantly altered by the acid treatment (Martinez-Sanz et al., 2011). The spectrum of BC and BCNWs shows a slight sharpening is observed especially in the broad band between 3000-3700  $\text{cm}^{-1}$ , and the bands 2920  $\text{cm}^{-1}$ , 1650  $\text{cm}^{-1}$  and 1420  $\text{cm}^{-1}$ , corresponding to OH stretching intramolecular hydrogen bonds, CH stretching, C=O stretching (carbonyl groups) and  $\text{CH}_2$  symmetric bending, respectively. Hence confirming the increase in the crystallinity index of the material (Martinez-Sanz et al., 2011).

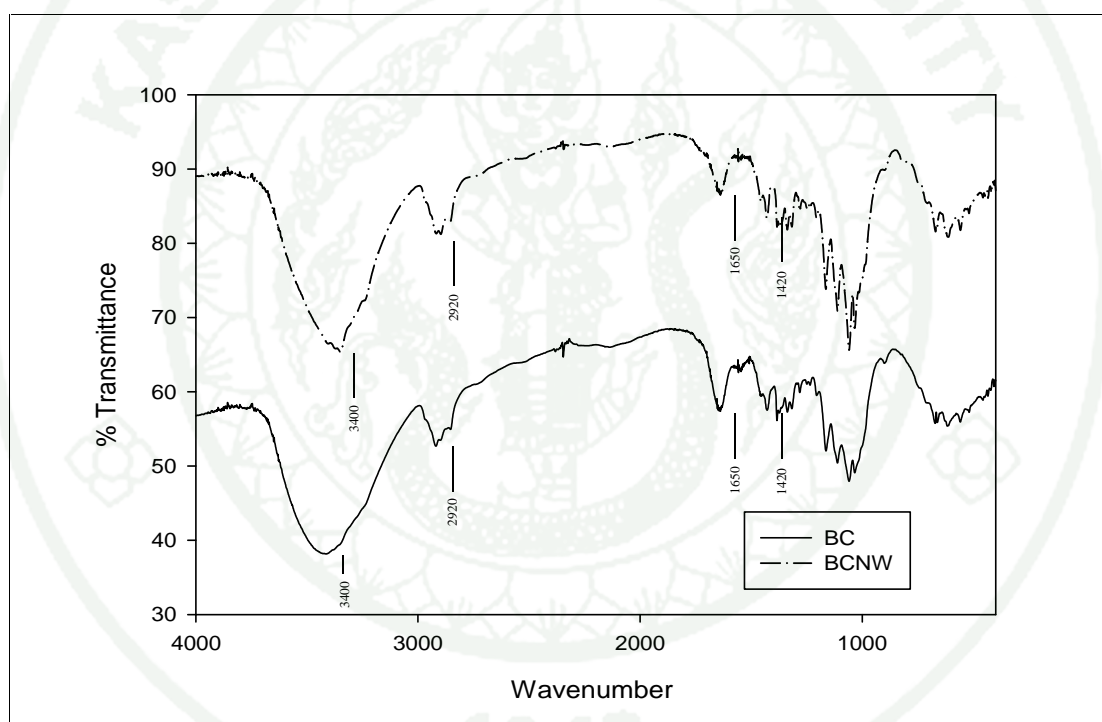


**Figure 18** FTIR spectra of native bacterial cellulose (BC) and nanowhiskers (BCNW).

#### 4. Thermogravimetric analysis of BC and BCNWs

The thermal stability of both BC and BCNWs was characterized using thermogravimetric analysis. In these experiments, the loss weight of the material was plotted as a function of temperature under air flow upon heating at 10  $^{\circ}\text{C min}^{-1}$ . The

thermal degradation temperature of BCNWs proceeded at lower temperatures than for the BC, as showed in table 7 and figure 19. This behavior was expected given that acid hydrolysis BCNWs have sulfate groups on the surface which induce the degradation of cellulose at lower thermal stability for BCNWs compared to native BC without sulfate groups (Wang *et al.*, 2007; Fahma *et al.*, 2010, 2011; Teixeira *et al.*, 2011).

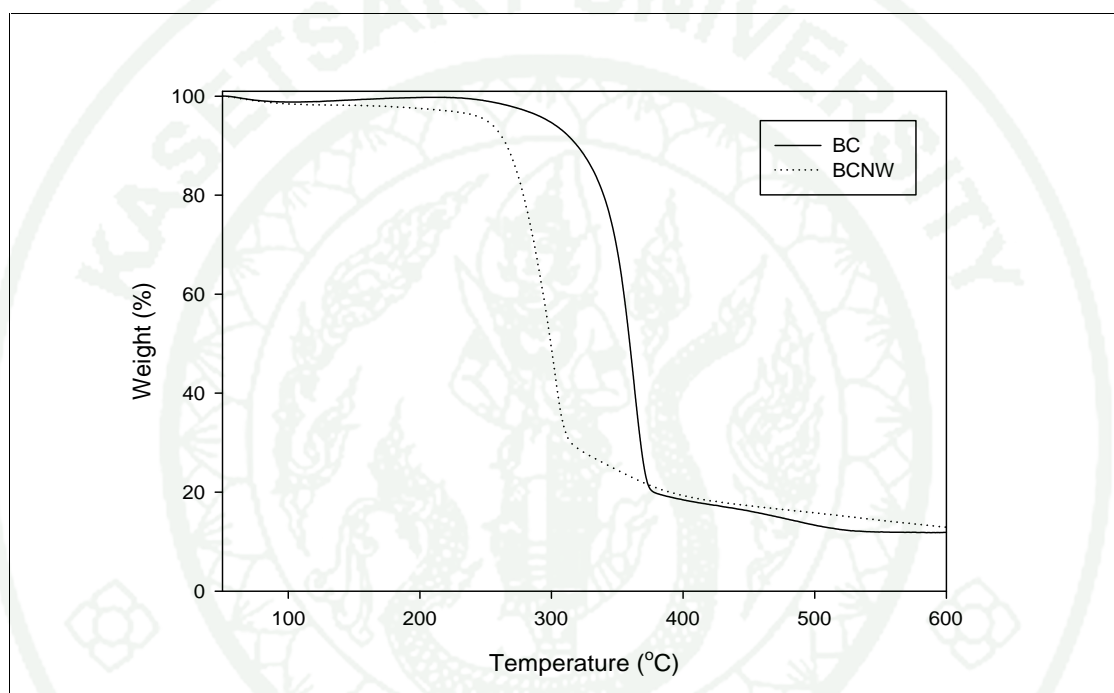


**Figure 19** TGA curves of BC and BCNWs.

**Table 7** Degradation onset temperature ( $T_o$ ), degradation temperature ( $T_d$ ) and corresponding weight loss (WL) of native bacterial cellulose (BC) and nanowhiskers (BCNWs).

Material	$T_o$ (°C)	$T_d$ (°C)	WL (%)
BC	350	364	88
BCNWs	280	302	87



### Study of bacterial cellulose/natural rubber composites

Bacterial cellulose/natural rubber composites were prepared by incorporation of BC at contents 5-20 phr into NR matrix with a laboratory two-roll mill. The effect of BC loading as filler on cure characteristics, mechanical properties, thermal properties and surface morphology were investigated in the filler loading range of 0-20 phr.

#### 5. Cure characteristics of BC/NR Composites

Table 8 shows the Mooney viscosity and cure characteristics for natural rubber compounds containing different proportions of BC. It can be seen that the Mooney viscosity increases with increasing filler loading. According to De *et al.* (2004) the presence of fibers increases the viscosity of the matrix. The increment in torque values with increasing fiber loading indicates that as more and more fiber gets into the matrix, the mobility of the macromolecular chains of the natural rubber decreases, resulting in a more rigid vulcanizate (De *et al.*, 2004). Also, the minimum torque gives an indication of the filler content in the natural rubber, while the maximum torque is a measure of crosslink density and stiffness in the natural rubber. This result was also observed by Lopattananon *et al.* (2011) The minimum torque, which is a measure of the initial viscosity of a rubber compound, is independent of fiber loading, but the maximum torque appears as a function of fiber concentration, indicating a rise in stiffness of the vulcanizate (Lopattananon *et al.*, 2006). In addition, the inclusion of fibers results in restricted mobility of the rubber molecules (Lopattananon *et al.*, 2006). Moreover, the torque difference ( $M_H - M_L$ ) values of vulcanizates also increase with fiber loading, which implies a higher degree of fiber and natural rubber matrix interaction. The scorch time was found to be independent of filler loading; however a gum compound was previously shown to exhibit higher scorch time. The cure time was not much affected by increasing amounts of filler.

**Table 8** Curing characteristics and mechanical properties of natural rubber and natural rubber/bacterial cellulose composites.

Parameter	Filler loading (phr)				
	BC0	BC5	BC10	BC15	BC20
Mooney viscosity (MU)	21.1	25.9	30.8	32.3	36.5
M <sub>L</sub> (dNm)*	0.46	0.55	0.74	0.81	0.96
M <sub>H</sub> (dNm)*	7.17	8.40	9.21	10.33	11.08
M <sub>H</sub> -M <sub>L</sub>	6.77	7.84	8.47	9.52	10.12
Scorch time (min)	10.32	10.60	10.43	9.94	9.77
Cure time (min)	15.84	15.96	15.94	15.47	15.95
Tensile strength (MPa)	20.4(0.67)	17.2(2.51)	14.0(0.43)	11.5(0.54)	8.75(0.31)
Elongation at break (%)	938.6(15.60)	824.2(10.15)	808.6(7.45)	723.5(7.07)	645.7(16.29)
Modulus at 100% (MPa)	0.75(0.04)	1.04(0.15)	1.20(0.03)	1.46(0.01)	1.65(0.01)
Modulus at 300% (MPa)	2.04(0.12)	2.56(0.39)	2.58(0.07)	3.21(0.07)	3.33(0.02)
Modulus at 500% (MPa)	4.47(0.37)	5.57(0.89)	5.41(0.10)	3.33(0.02)	6.37(0.02)
Tear strength (MPa)	28.8	26.9	28.2	31.2	31.6
Hardness (Shore A)	36	43	47	52	55

\* M<sub>H</sub> = maximum torque, M<sub>L</sub> = minimum torque, the number given in parentheses are the standard deviations.

## 6. Mechanical Properties of BC/NR Composites

The effects of filler loading on tensile strength, elongation at break, modulus, tear strength and hardness of natural rubber and BC/NR composites are shown in Table 8. Typical stress-strain curves are shown in Figure 20. These curves clearly show the effect of filler on the mechanical properties of composites. The neat NR matrix and BC/NR composites exhibit an elastic non-linear behavior typical for amorphous polymers at  $T > T_g$  (Jacob *et al.*, 2010). The stress regularly increases slightly and remains more or less constant up to the fracture of the composites (Jacob *et al.*, 2010). At higher filler content, the tensile behaviors become significantly different. The composites exhibit a stiffer and brittle behavior (Jacob *et al.*, 2010). Tensile strength and elongation at break are higher for neat NR than for BC/NR composites. Tensile strength and elongation at break of BC/NR composites illustrate a decreasing trend with increasing filler loading. This result may be due to the size and geometrical factors (length and shape) of the filler, whereby an irregularly shaped filler tends to decrease the strength of composites due to poor adhesion or incompatibility between hydrophilic BC and hydrophobic NR (Ismail *et al.*, 2002). This leads to the filler's inability to support the uniform transmission of stress from the rubber (Ismail *et al.*, 2002). However, the percentage of decrement values of tensile strength and elongation at break of BC/NR composites were lower than for other fibers such as grass (De *et al.*, 2004), pineapple leaf (Lopattananon *et al.*, 2006), bamboo (Ismail *et al.*, 2002), etc. This is because BC is practically pure cellulose, with ribbon-shaped fibrils less than 100 nm wide (Martinez-Sanz *et al.*, 2011). Hardness and modulus at 100%, 300% and 500% of neat NR and BC/NR composites increased with increasing filler loading, whereas the opposite trend can be observed for the elongation at break of a BC-filled NR matrix. De *et al.* (2004) and Ismail *et al.* (2002) also obtained similar results in their work on other filled compounds. Filler may restrict the movement of NR matrix macromolecules, leading to a reduction of resistance to break of the composites. Tear strength of NR and BC/NR composites increased with increasing filler loading. This is in agreement with Bipinbal and Kutty (2008) who worked on short nylon fiber/natural rubber composites. BC fibers are oriented perpendicular to the crack propagation; as the BC content increases there will

be more and more hindrance to crack propagation, as is evident from the increase in tear strength of the composites.

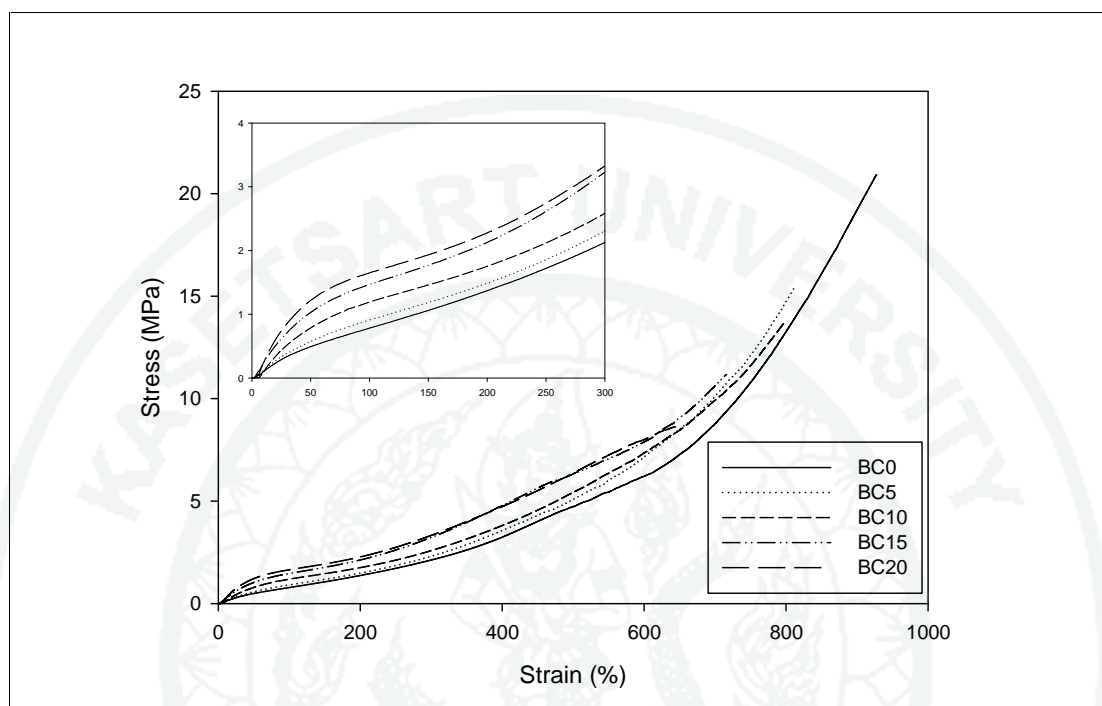


**Figure 20** Typical stress-strain curves obtained from tensile test for NR vulcanizate and BC/NR composites.

## 7. Differential Scanning Calorimeter of BC/NR Composites

DSC measurements were carried out for all compositions in order to study the influence of BC content on glass transition temperature ( $T_g$ ) of the NR matrix as shown in table 9.  $T_g$  was located around  $-61\text{ }^{\circ}\text{C}$  for neat natural rubber and  $-60\text{ }^{\circ}\text{C}$  for rubber filled with 5–20 phr bacterial cellulose. These results showed that BC had no significant effect on  $T_g$  values of BC/NR composites. This is in agreement with Bras *et al.* (2010) observations of cellulose whisker-filled composites, where no modification of  $T_g$  values was reported with an increasing amount of whiskers, regardless of the nature of the polymer matrix (Bras *et al.*, 2010).

**Table 9** Glass transition temperature of BC/NR composites from differential scanning calorimeter.

Bacterial cellulose loading (phr)	Glass transition temperature (°C)
0	-61.39
5	-59.49
10	-60.08
15	-59.62
20	-60.04

## 8. Dynamic mechanical properties of BC/NR Composites

Dynamic mechanical analyses of neat NR and composites reinforced with 2-15 % (w/w) BC were indicated in the Fig. 21 and 22 for log E' (storage modulus) and the plot of tan  $\delta$  (damping factor) at 1 Hz as a function of temperature.

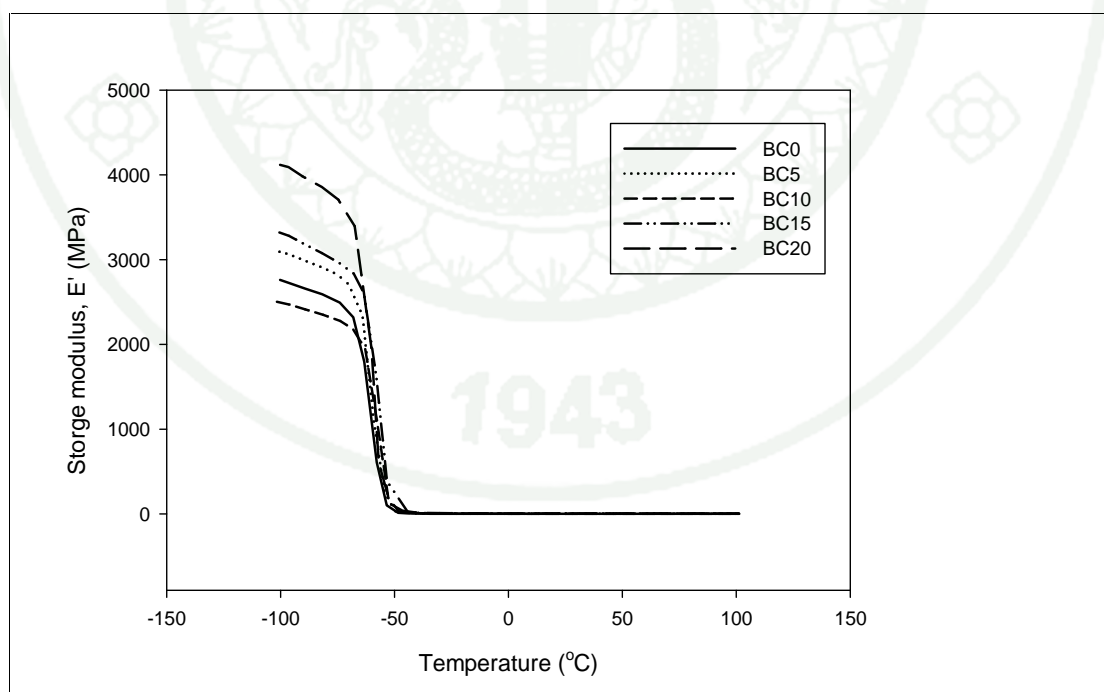


**Figure 21** storage modulus (E') & temperature curve at 1 Hz of BC/NR composites.



At low temperature storage modulus even below glass transition temperature is good attest for strong reinforcing tendency of BC in the NR matrix (Gopalan *et al.*, 2003). The composites containing BC exhibited an increase the storage modulus compared to the neat NR. The storage modulus mainly depends on the stiffness and rigidity of composites. According to Jacob *et al.* (2010) any factors that increase the stiffness of the system will result in an increase in the storage modulus. Typically, neat NR, composed of only the rubber phase (fully amorphous phase), give the material more flexibility, which result in a low degree of stiffness and low storage modulus. When BC was incorporated into the rubber matrix, the stiffness of the composite increased, this resulted in a high storage modulus (Srisuwan *et al.*, 2011). The values of storage modulus decrease sharply after -54 to -46 °C (for different compound) as a result of the glass transition phenomenon. The glassy region the components are in a frozen state and are highly immobile. But above -30 °C the values of storage modulus became almost constant. Geethamma *et al.* (2005) and Joseph *et al.* (2010) explained that on increasing temperature the value of storage modulus decreases until it stabilizes and coincides with the elastic zone of material (Geethamma *et al.*, 2005). Because of the matrix become more mobile and loses its close packing arrangement and as a result the modulus decrease (Wongsorat *et al.*, 2011). It is interesting that the transition between the glass and elastic zone is more prominent for BC reinforce NR composites compared to that for gum and so the modulus drop is higher for the former (Geethamma *et al.*, 2005).

1943

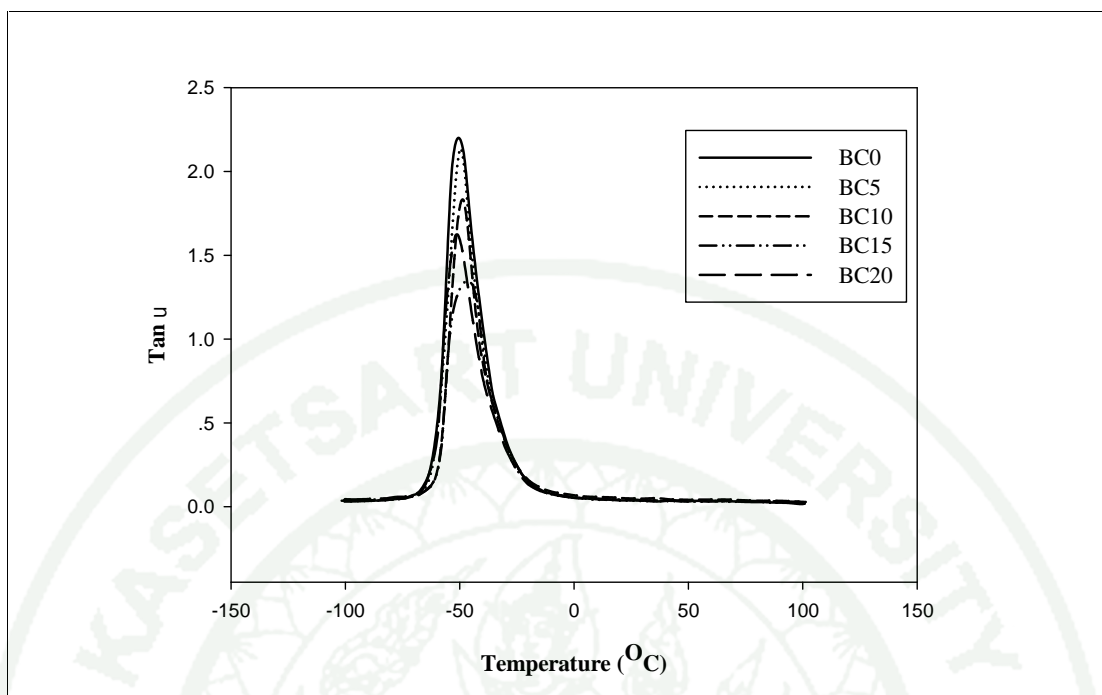


**Figure 22** Tan  $\delta$  versus temperature curve at 1 Hz of BC/NR composites.

The variation in tan  $\delta$  with temperature can be seen in figure 22. The result show that the intensity of the relaxation process was highest for neat NR which indicating a large degree of molecular mobility. The damping peak of composites showed a decreased peak height with upon reinforcement with BC and is clearly shown in Table 10. This can also be attributed to the decrease of matrix material amount, which is responsible for damping properties, which is possibly an outcome of restriction of molecular mobility of NR polymer chain in the proximity of BC (Visakh *et al.*, 2012). Jacob *et al.* (2010) and Joseph *et al.* (2010) also reported that the incorporation of BC acted as restricted the mobility of rubber chains, which chain elasticity is blocking, leading to lower flexibility (higher rigidity), lower degree of molecular motion and lower damping characteristic. Another reason for the decrease was that there was less matrix by volume to dissipate the mechanical energy (Srisuwan *et al.*, 2011; Wongsorat *et al.*, 2011).

**Table 10** Peak height and Tg from  $\tan \delta$  of bacterial cellulose/natural rubber composites.

Bacterial cellulose loading (phr)	Peak height ( $\tan \delta_{\max}$ )	$\tan \delta_{\max}$ (Tg)
0	2.1	-48.4
5	2.1	-49.7
10	1.8	-48.1
15	1.3	-44.1
20	1.6	-51.8

### 9. Scanning electron microscopy of BC/NR Composites

SEM photographs of the fracture surfaces of natural rubber reinforced with 5–20 phr bacterial cellulose at a magnification of 350X are shown in Figures 23. The BC/NR composites exhibit a more homogeneous surface than composites using other fibers as filler, such as sisal/oil palm hybrid fiber (Jacob *et al.*, 2004), bamboo fiber (Ismail *et al.*, 2002), rattan (Muniandy *et al.*, 2011), rice husk (Srisuwan *et al.*, 2011), sisal fiber (Wongsorat *et al.*, 2011) and grass fiber (Juntuek *et al.*, 2010). Morphological analysis indicated that BC can be found in various shapes, sizes and lengths. In addition, it can be seen that there was low pull-out of fibers on the fracture surface, a few voids left after the fibers were pulled out from the matrix, and small gaps between the BC particles and the NR matrix. These results indicated that the incorporation of bacterial cellulose into the natural rubber matrix enhanced the hardness and modulus of composites.

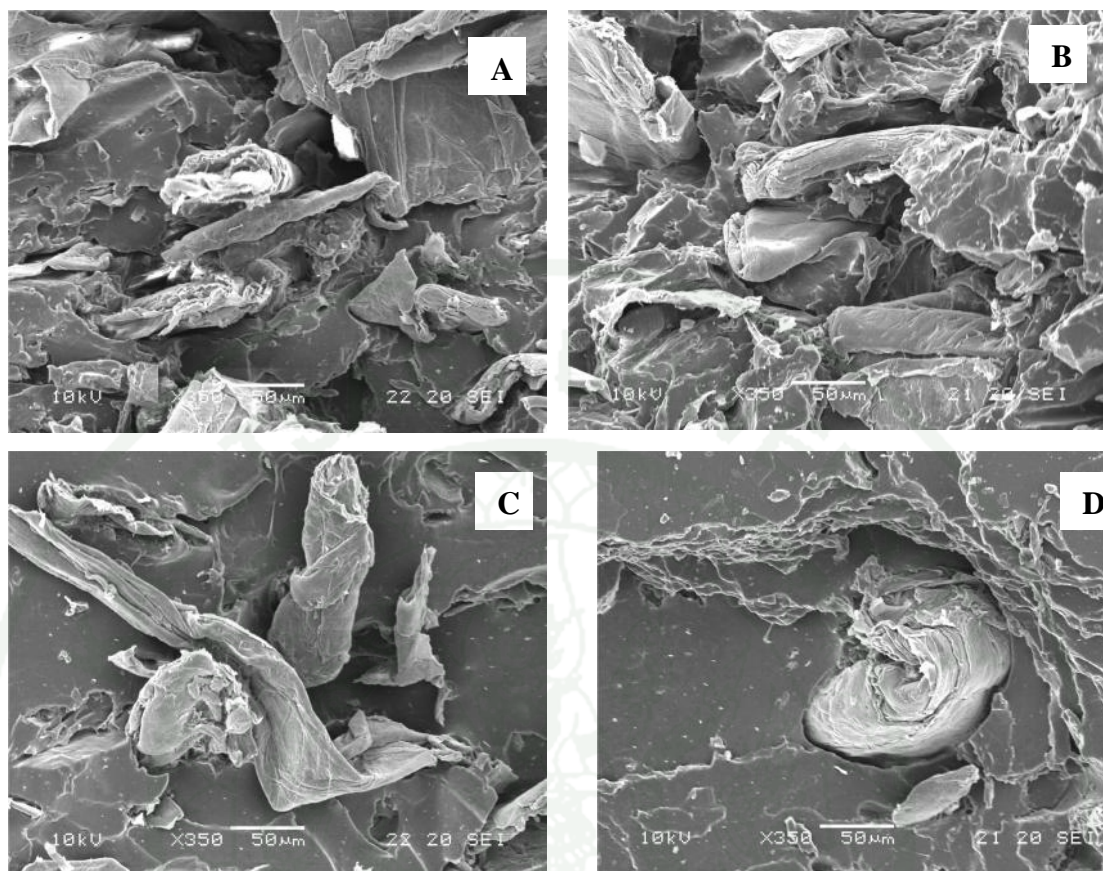


**Figure 23** SEM photograph of fracture surface of the natural rubber reinforce with 5, 10, 15 and 20 phr bacterial cellulose at magnification of 350X : (A) 5 phr (B) 10 phr (C) 15 phr (D) 20 phr.

1943



### Study of BCNWs/natural rubber nanocomposites

BCNWs were used as the reinforcing phase to prepare nanocomposite films by casting/evaporation using latex of natural rubber as the matrix. The effects of BCNWs loading as filler on mechanical properties, thermal properties and morphology were investigated in the filler loading range of 0-15% wt.

#### 10. Tensile properties of BCNWs/NR nanocomposites

Mechanical properties in terms of tensile strength, elongation percentage and modulus of BCNWs/NR nanocomposites were evaluated as a function of BCNWs content. All the results were also compared with neat NR as shown in table 11. The tensile strength and young modulus of the nanocomposites was increased 2.5 fold and 3.5 fold, respectively (with 7.5% BCNWs) and elongation at break decrease 1.7 fold (with 7.5% BCNWs). At BCNWs content of 7.5 %wt, the tensile strength is highest. This result may be due to some agglomerations of the fibers at higher loading which will act as points of weakness, thus leading to early breakdown of the composites (Bipinbal and Kutty, 2008). While, young modulus of BCNWs/NR nanocomposites increased with increasing filler content, whereas the opposite trend can be observed for the elongation at break of BCNWs fill NR. Bras *et al.* (2010) and Siqueira *et al.* (2010c) also obtained similar results in their work of other filler nanocomposites. It is due to BCNWs agglomerations at higher fiber contents, cause more fiber-fiber interactions than matrix-fiber interactions. This can result in easier pullout of the fibers from the matrix at high strains. The resulting voids act as defects inducing earlier breakage of the composites and thus reducing elongation at break (Bipinbal and Kutty, 2008).

Typical stress vs strain curves for the studied materials are shown in figure 24. Stress-strain curves clearly show the stiffening effect of BCNWs on NR nanocomposites films as seen from increased initial slopes of the curves. The stress-strain curves behavior of BCNWs/NR nanocomposites was significantly different from that neat NR. At low filler content, the material exhibit an elastic nonlinear



behavior typical for amorphous polymer at  $T > T_g$ . The stress regularly slightly increases and remain more or less constant up to the fracture of the films. At higher filler content, the materials exhibit a brittle behavior (Bendahou *et al.*, 2010).

**Table 11** Tensile properties of the nanocomposites in comparison with matrix.

Sample	Tensile strength (MPa)	Elongation at break (%)	Young's modulus (MPa)
BCNWs0	1.79±0.1	870.69±42	0.34±0.08
BCNWs2.5	1.95±0.2	744.20±86	0.42±0.08
BCNWs5	2.81±0.4	716.92±94	0.61±0.05
BCNWs7.5	4.46±0.1	667.78±78	0.81±0.06
BCNWs10	2.53±0.3	518.57±32	0.78±0.05
BCNWs15	4.12±0.3	500.61±21	1.18±0.04

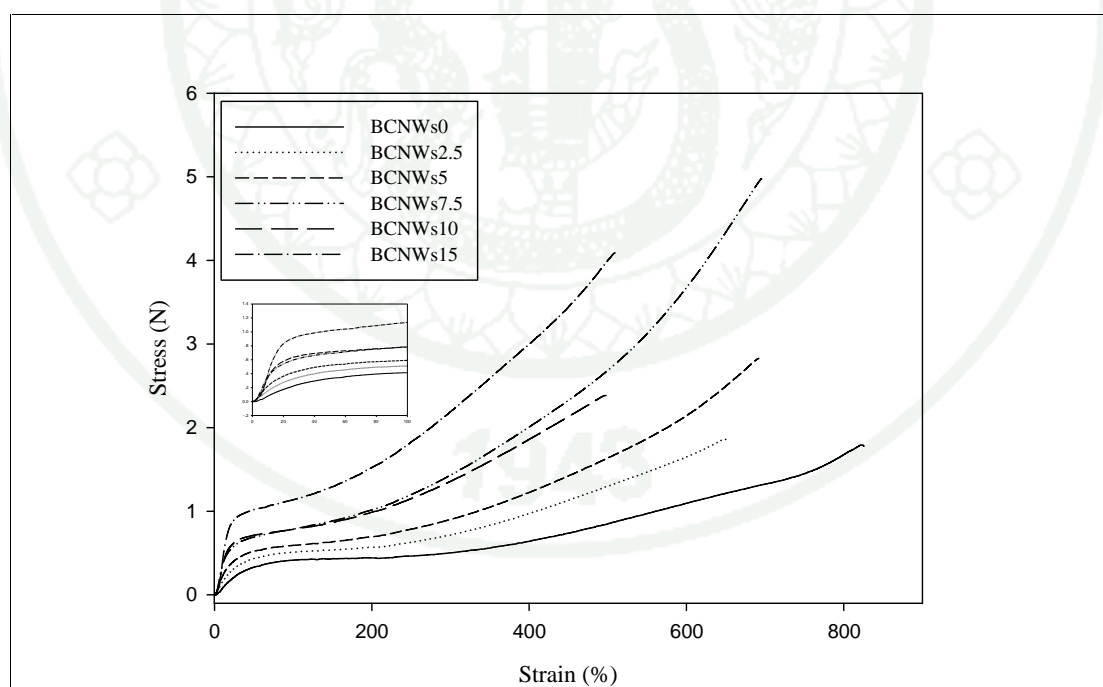


**Figure 24** Typical stress-strain curves obtained from tensile test for BCNWs/NR nanocomposites.

## 11. Differential Scanning Calorimeter of BCNWs/NR nanocomposites

The effect of addition of BCNWs on glass transition temperature ( $T_g$ ) of BCNWs/NR nanocomposites were carried out by differential scanning calorimeter and compared to that of neat NR matrix. The glass transition temperature of all nanocomposites was located range -60 to -62 °C, as showed in figure 25. Bras *et al* (2010) and Bendahou *et al* (2010) also obtained similar results in their work of sugarcane bagasse whiskers and cellulose whiskers extracted from the rachis of date palm tree, respectively filled NR nanocomposites. It is known that the glass transition ( $T_g$ ) is a complex phenomenon which depends on several factors including intermolecular interactions, steric effects, the chain flexibility, the molecular weight, the branching and the cross-linking density (Frone *et al.*, 2013). Therefore, BCNWs filled composites where no modification of  $T_g$  values when increasing the amount of whiskers regardless the nature of the polymer matrix (Bras *et al.*, 2010).

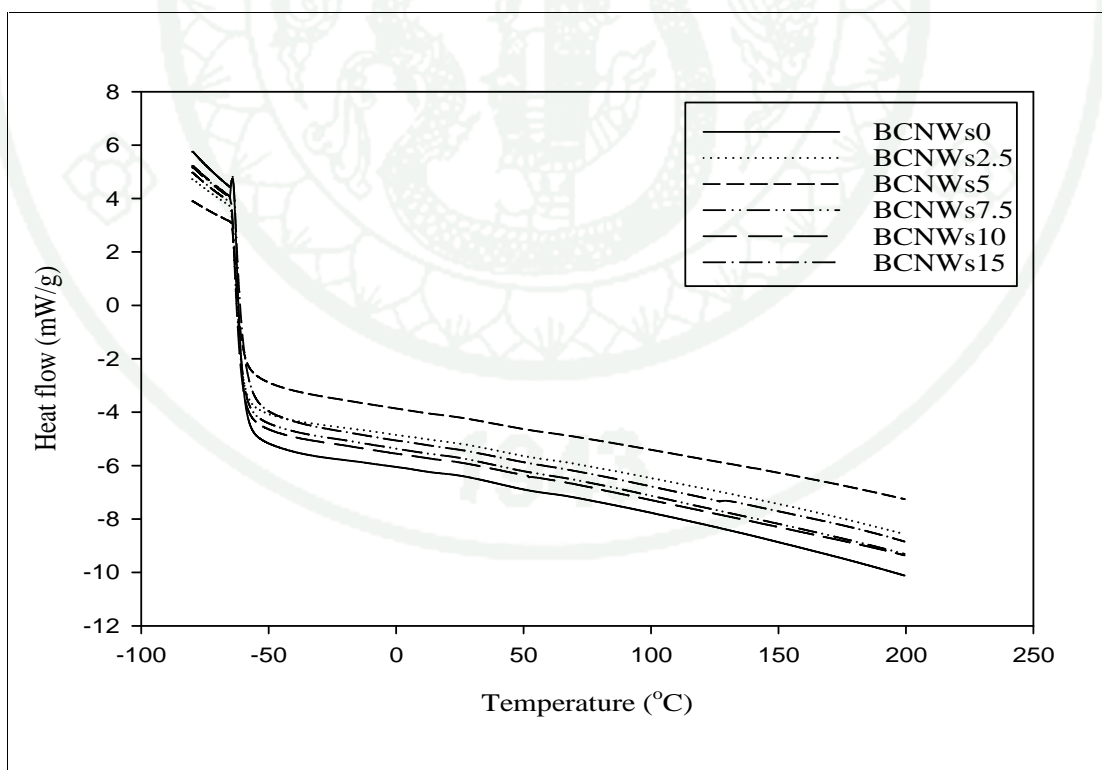


**Figure 25** DSC thermograms of NR and BCNWs/NR nanocomposites.

## 12. Thermo gravimetric analysis of BCNWs/NR nanocomposites

Thermo gravimetric analysis (TGA) measures the change in weight of the material when it is heated in the presence of air. When a rubber compound is heated at lower temperature, volatile components like moisture will get evaporated first. On heating further, the polymer part will degrade and get converted into gaseous products; a corresponding loss in weight is reflected in the curve. Further heating will remove all organic matter, giving the weight of inorganic fillers in the compound (Visakh *et al.*, 2012). The results shown that no significant effect of the BCNWs on degradation temperature of NR whereas the onset temperature was slightly changed. Figure 26 shows the TGA analysis of the neat NR and BCNWs/NR nanocomposites samples. BCNWs/NR nanocomposites indicated that slightly lower onset degradation temperature than neat NR for all BCNWs/NR nanocomposites with increasing BCNWs content. The lower onset degradation in case of BCNWs/NR nanocomposites could be due to the lower onset degradation temperature of BCNWs than NR (Bras *et al.*, 2010). Figure 27 shows that the DTG curve of the neat NR and nanocomposites with different percentages of BCNWs. According to the derivative TGA curves of neat NR and BCNWs/NR nanocomposites exhibited degradation peak at 380 °C.

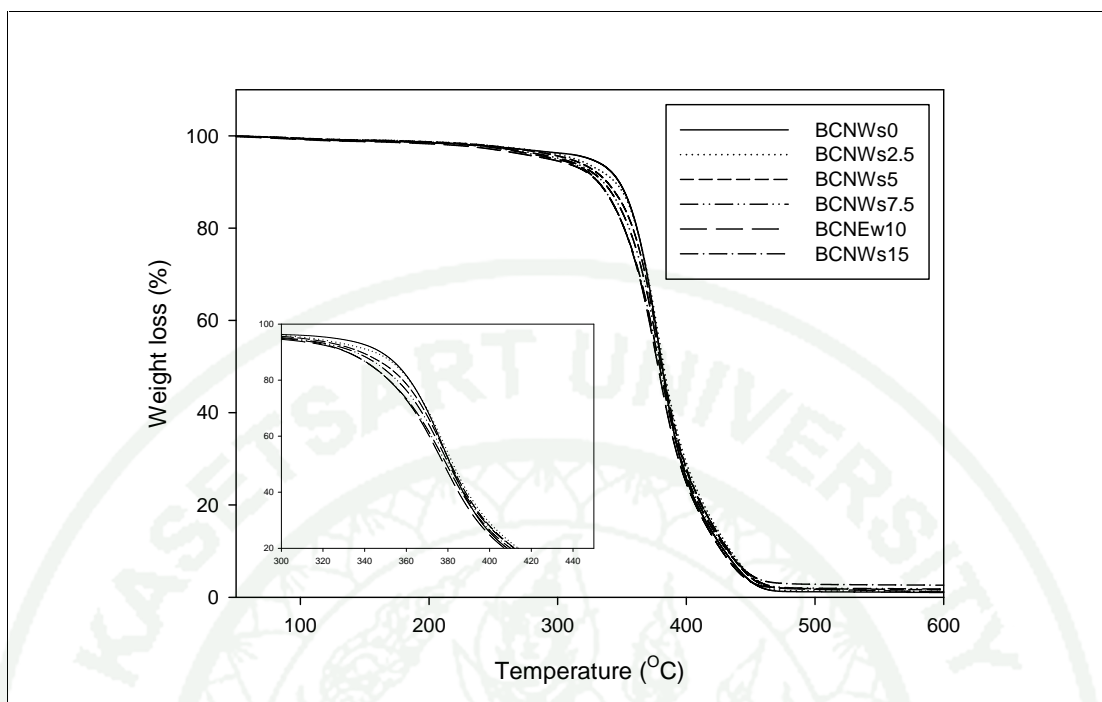


**Figure 26** TGA curve of neat NR and BCNWs/NR nanocomposites

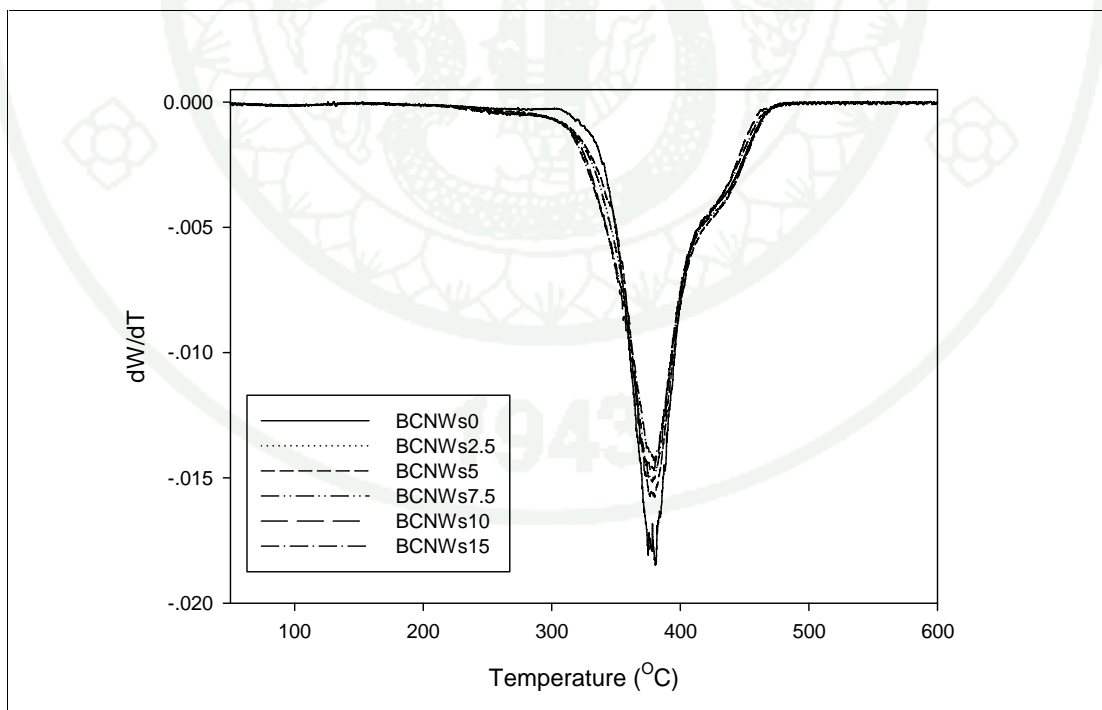


**Figure 27** DTG curve of neat NR and BCNWs/NR nanocomposites

## 12. Morphological analysis of BCNWs/NR nanocomposites

The morphological investigation of BCNWs/NR nanocomposites was performed using SEM observations. Figure 28 shows the fractured surface of the neat NR matrix and BCNWs/NR nanocomposites. The fracture surface of neat NR was similar to nanocomposites containing BCNWs, expect for a slight increase in surface roughness with the addition of BCNWs.

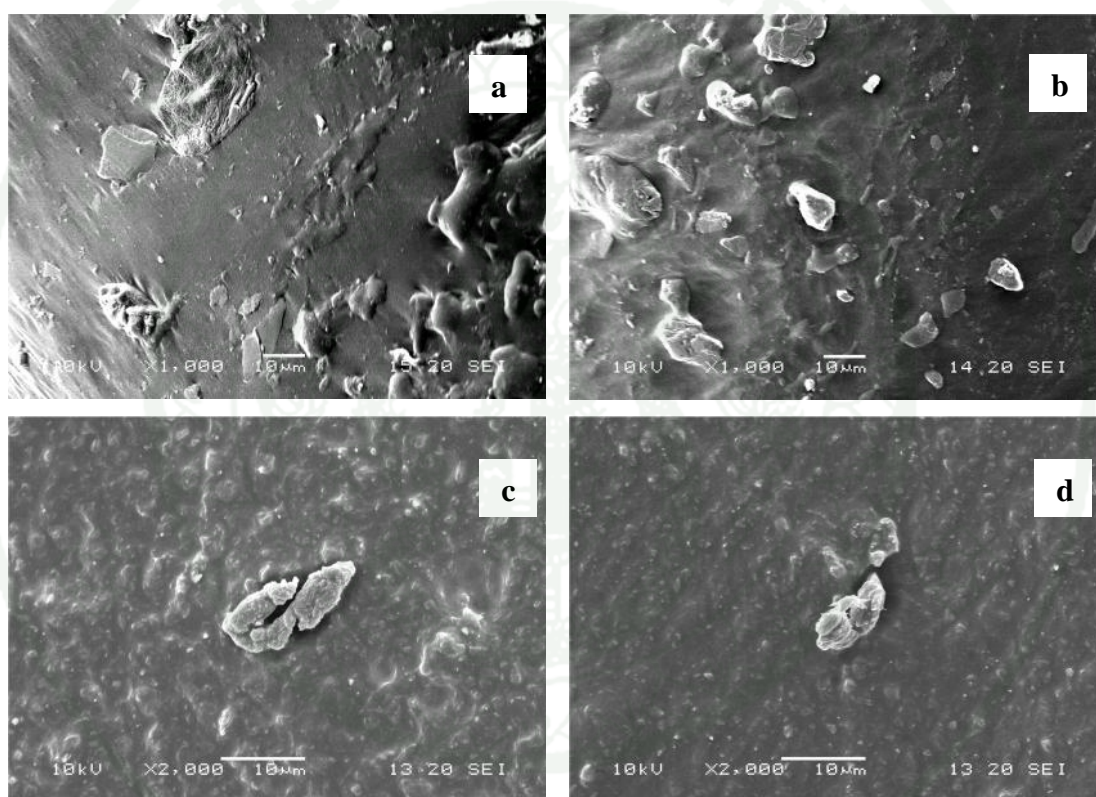


**Figure 28** SEM of fracture surfaces of NR base films reinforced with BCNWs : (a) neat NR (b) NR-BC2.5 (c) NR-BCNWs10 (d) NR-BCNWs15.



## CONCLUSION

Bacterial cellulose powder showed a particle size of 180  $\mu\text{m}$  and BCNWs have an average length, diameter and aspect ratio of 186 nm, 7 nm, and 28, respectively. BCNWs were successfully prepared from bacterial cellulose powder by acid hydrolysis. BC powder was used as the reinforcing phase in vulcanized NR, while BCNWs were used as the reinforcing phase in latex of NR.

The incorporation of bacterial cellulose fillers has increased the Mooney viscosity, maximum torque, minimum torque, modulus at 100%, 300%, 500%, tear strength and hardness. However, tensile strength and elongation at break of BC/NR composites decreased with increase BC content. SEM micrographs showed that BC and NR had low interfacial adhesion which caused the decrement of tensile strength of BC/NR composites to a certain degree. Nevertheless, bacterial cellulose can be used as filler depending on the performance desired for a given application, for instance, application that requires moderate tensile properties.

BCNWs were used as reinforcing elements in NR latex. The effect of BCNWs loading on tensile properties and thermal properties was investigated. Tensile strength increased up to 7.5% (wt%) BCNWs and then decreased. Modulus increased, while elongation at break decreased with increasing BCNWs loading. The study on thermal properties was carried out by DSC and TGA. The results showed that no change of the glass transition temperature ( $T_g$ ) degradation temperature. SEM was used to determine the dispersion of filler in rubber matrix, the fine dispersion of BCNWs in the rubber matrix can be observed.

## LITERATURE CITED

- Alemдар, A. and M. Sain. 2008a. Biocomposites from Wheat Straw Nanofibers: Morphology, Thermal and Mechanical Properties. **Compos Sci Technol.** 68(2): 557-565.
- \_\_\_\_\_. 2008b. Isolation and Characterization of Nanofibers from Agricultural Residues – Wheat Straw and Soy Hulls. **Bioresource technology.** 99(6): 1664-1671.
- Azizi Samir, M.A.S., F. Alloin and A. Dufresne. 2005. Review of Recent Research into Cellulosic Whiskers, Their Properties and Their Application in Nanocomposite Field. **Biomacromolecules.** 6(2): 612–626.
- Barud, H.S., J.L. Souza, D.B. Santos, M.S. Crespi, C.A. Ribeiro, Y. Messaddeq and S.J.L. Ribeiro. 2011. Bacterial Cellulose/Poly(3-Hydroxybutyrate) Composite Membranes. **Carbohyd Polym.** 83(3): 1279-1284.
- Belbekhouche, S., J. Bras, G. Siqueira, C. Chappey, L. Lebrun, B. Khelifi, S. Marais and A. Dufresne. 2011. Water Sorption Behavior and Gas Barrier Properties of Cellulose Whiskers and Microfibrils Films. **Carbohyd Polym.** 83(4): 1740-1748.
- Bendahou, A., H. Kaddami and A. Dufresne. 2010. Investigation on the Effect of Cellulosic Nanoparticles' Morphology on the Properties of Natural Rubber Based Nanocomposites. **Eur Polym J.** 46(4): 609–620.
- Bendahou, A., Y. Habibi, H. Kaddami and A. Dufresne. 2009. Physico-Chemical Characterization of Palm from Phoenix Dactylifera-L, Preparation of Cellulose Whiskers and Natural Rubber-Based Nanocomposites. **J Biobased Mater Bio.** 3(1): 81-90.

- Bielecki, S., A. Krystynowicz, M. Turkiewicz and H. Kalinowska. 2002. Bacterial Cellulose, 37-90 pp. *In* E. J. Vandamme, S. De Baets and A. Steinbuechel. **Biopolymers Volume 5 Polysaccharides I, Polysaccharides from Ptokaryotes**. Wiley-VCH, Germany.
- Bipinbal, P.K. and S.K.N. Kutty. 2008. A Comparative Study of Short Nylon Fiber-Natural Rubber Composites Prepared from Dry Rubber and Latex Masterbatch. **J Appl Polym Sci**. 109(3): 1484-1491.
- Bondeson, D. and K. Oksman. 2007. Polylactic Acid/Cellulose Whisker Nanocomposites Modified by Polyvinyl Alcohol. **Composites Part A**. 38(12): 2486-2492.
- Bras, J., M.L. Hassan, C. Bruzesse, E.A. Hassan, N.A. El-Wakil and A. Dufresne. 2010. Mechanical, Barrier, and Biodegradability Properties of Bagasse Cellulose Whiskers Reinforced Natural Rubber Nanocomposites. **Ind Crop Prod**. 32(3): 627-633.
- Brinchi, L., F. Cotana, E. Fortunati and J.M. Kenny. 2013. Production of Nanocrystalline Cellulose from Lignocellulosic Biomass: Technology and Applications. **Carbohydr Polym**. 94(1): 154-169.
- Chen, D., D. Lawton, M.R. Thompson and Q. Liu. 2012. Biocomposites Reinforced with Cellulose Nanocrystals Derived from Potato Peel Waste. **Carbohydr Polym**. 90(1): 709-716.
- Chen, W., H. Yu, Y. Liu, P. Chen, M. Zhang and Y. Hai. 2011. Individualization of Cellulose Nanofibers from Wood Using High-Intensity Ultrasonication Combined with Chemical Pretreatments. **Carbohydr Polym**. 83(4): 1804-1811.

- Chen, Y., C.H. Liu, P.R. Chang, X.D. Cao and D.P. Anderson. 2009. Bionanocomposites Based on Pea Starch and Cellulose Nanowhiskers Hydrolyzed from Pea Hull Fibre: Effect of Hydrolysis Time. **Carbohydr Polym.** 76(4): 607-615.
- Cherian, B.M., L.A. Pothan, T. Nguyen-Chung, G. Mennig, M. Kottaisamy and S. Thomas. 2008. A Novel Method for the Synthesis of Cellulose Nanofibril Whiskers from Banana Fibers and Characterization. **Journal of agricultural and food chemistry.** 56(14): 5617-5627.
- Corrêa, A.C., E.M. Teixeira, L.A. Pessan and L.H.C. Mattoso. 2010. Cellulose Nanofibers from Curaua Fibers. **Cellulose.** 17(6): 1183-1192.
- De, D., D. De and B. Adhikari. 2004. The Effect of Grass Fiber Filler on Curing Characteristics and Mechanical Properties of Natural Rubber. **Polym Advan Technol.** 15(12): 708-715.
- Deepa, B., E. Abraham, B.M. Cherian, A. Bismarck, J.J. Blaker, L.A. Pothan, A.L. Leao, S.F.d. Souza and M. Kottaisamy. 2011. Structure, Morphology and Thermal Characteristics of Banana Nano Fibers Obtained by Steam Explosion. **Bioresource technology.** 102(2): 1988-1997.
- Fahma, F., S. Iwamoto, N. Hori, T. Iwata and A. Takemura. 2010. Isolation, Preparation, and Characterization of Nanofibers from Oil Palm Empty-Fruit-Bunch (Opefb). **Cellulose.** 17(5): 977-985.
- \_\_\_\_\_. 2011. Effect of Pre-Acid-Hydrolysis Treatment on Morphology and Properties of Cellulose Nanowhiskers from Coconut Husk. **Cellulose.** 18(2): 443-450.

- Flauzino Neto, W.P., H.A. Silvério, N.O. Dantas and D. Pasquini. 2013. Extraction and Characterization of Cellulose Nanocrystals from Agro-Industrial Residue – Soy Hulls. **Ind Crop Prod.** 42(480–488.
- Gabr, M.H., M.A. Elrahman, K. Okubo and T. Fujii. 2010. A Study on Mechanical Properties of Bacterial Cellulose/Epoxy Reinforced by Plain Woven Carbon Fiber Modified with Liquid Rubber. **Compos Part a-Appl S.** 41(9): 1263-1271.
- Gardner, D.J., G.S. Oporto, R. Mills and M.A.S.A. Samir. 2008. Adhesion and Surface Issues in Cellulose and Nanocellulose. **J Adhes Sci Technol.** 22(5-6): 545-567.
- Geethamma, V.G., G. Kalaprasad, G. Groeninckx and S. Thomas. 2005. Dynamic Mechanical Behavior of Short Coir Fiber Reinforced Natural Rubber Composites. **Compos Part a-Appl S.** 36(11): 1499-1506.
- George, J., K.V. Ramana, A.S. Bawa and Siddaramaiah. 2011. Bacterial Cellulose Nanocrystals Exhibiting High Thermal Stability and Their Polymer Nanocomposites. **Int J Biol Macromol.** 48(1): 50-57.
- Gindl, W. and J. Keckes. 2004. Tensile Properties of Cellulose Acetate Butyrate Composites Reinforced with Bacterial Cellulose. **Compos Sci Technol.** 64(15): 2407-2413.
- Grande, C.J., F.G. Torres, C.M. Gomez, O.P. Troncoso, J. Canet-Ferrer and J. Martinez-Pastor. 2009. Development of Self-Assembled Bacterial Cellulose-Starch Nanocomposites. **Mat Sci Eng C-Bio S.** 29(4): 1098-1104.
- Haiyuan, P. 2006. **Microbial-Derived Cellulose-Reinforced Biocomposites.** Master Thesis, University of Canterbury.



- Hashaikeh, R. and H. Abushammala. 2011. Acid Mediated Networked Cellulose: Preparation and Characterization. **Carbohydr Polym.** 83(3): 1088-1094.
- Hu, L., Y.Z. Wan, F. He, H.L. Luo, H. Liang, X.L. Li and J.H. Wang. 2009. Effect of Coupling Treatment on Mechanical Properties of Bacterial Cellulose Nanofibre-Reinforced Upr Ecocomposites. **Mater Lett.** 63(22): 1952-1954.
- Ismail, H., M.R. Edyham and B. Wirjosentono. 2002. Bamboo Fibre Filled Natural Rubber Composites: The Effects of Filler Loading and Bonding Agent. **Polym Test.** 21(2): 139-144.
- Jacob, M., S. Thomas and K.T. Varughese. 2004. Mechanical Properties of Sisal/Oil Palm Hybrid Fiber Reinforced Natural Rubber Composites. **Compos Sci Technol.** 64(7-8): 955-965.
- Jacob, M., J. Jose, S. Jose, K.T. Varughese and S. Thomas. 2010. Viscoelastic and Thermal Properties of Woven-Sisal-Fabric-Reinforced Natural-Rubber Biocomposites. **J Appl Polym Sci.** 117(1): 614-621.
- John, M.J. and S. Thomas. 2008. Biofibres and Biocomposites. **Carbohydr Polym.** 71(3): 343-364.
- \_\_\_\_\_. 2010. Cellulosic Fibril-Rubber Nanocomposites, 197-208 pp. *In* S. Thomas and R. Stephen. **Rubber Nanocomposites: Preparation, Properties and Applications.** John Wiley & Sons, United State of America.
- Jose, J.P., S.K. Malhotra, S. Thomas, K. Joseph, K. Goda and M.S. Sreekala. 2012. Advances in Polymer Composites: Macro- and Microcomposites – State of the Art, New Challenges, and Opportunities, 1-16 pp. *In* S. Thomas, K. Joseph, S. K. Malhotra, K. Goda and M. S. Sreekala. **Polymer Composites: Volume 1, First Edition.** Wiley-VCH Verlag GmbH & Co. KGaA.

- Joseph, S., S.P. Appukuttan, J.M. Kenny, D. Puglia, S. Thomas and K. Joseph. 2010. Dynamic Mechanical Properties of Oil Palm Microfibril-Reinforced Natural Rubber Composites. **J Appl Polym Sci.** 117(3): 1298-1308.
- Juntuek, P., C. Ruksakulpiwat, P. Chumsamrong and Y. Ruksakulpiwat. 2010. Mechanical Properties of Polylactic Acid and Natural Rubber Blends Using Vetiver Grass Fiber as Filler. **Advanced Materials Research.** 123 - 125(1167-1170).
- Kaushik, A. and M. Singh. 2011. Isolation and Characterization of Cellulose Nanofibrils from Wheat Straw Using Steam Explosion Coupled with High Shear Homogenization. **Carbohydr Res.** 346(1): 76-85.
- Kaushik, A., M. Singh and G. Verma. 2010. Green Nanocomposites Based on Thermoplastic Starch and Steam Exploded Cellulose Nanofibrils from Wheat Straw. **Carbohydr Polym.** 82(2): 337-345.
- Klemm, D., B. Heublein, H.-P. Fink and A. Bohn. 2005. Cellulose: Fascinating Biopolymer and Sustainable Raw Material. **Angew Chem Int Edit.** 44(22): 3358-3393.
- Klemm, D., D. Schumann, F. Kramer, N. Hessler, M. Hornung, H.P. Schmauder and S. Marsch. 2006. Nanocelluloses as Innovative Polymers in Research and Application. **Adv Polym Sci.** 205(49-96).
- Klemm, D., F. Kramer, S. Moritz, T. Lindström, M. Ankerfors, D. Gray and A. Dorris. 2011. Nanocelluloses: A New Family of Nature-Based Materials. **Angew Chem Int Edit.** 50(24): 5438-5466.
- Lavoine, N., I. Desloges, A. Dufresne and J. Bras. 2012. Microfibrillated Cellulose - Its Barrier Properties and Applications in Cellulosic Materials: A Review. **Carbohydr Polym.** 90(2): 735-764.

- Lee, B.H., H.J. Kim and H.S. Yang. 2012. Polymerization of Aniline on Bacterial Cellulose and Characterization of Bacterial Cellulose/Polyaniline Nanocomposite Films. **Curr Appl Phys.** 12(1): 75-80.
- Lopattananon, N., D. Jitkalong and M. Seadan. 2011. Hybridized Reinforcement of Natural Rubber with Silane-Modified Short Cellulose Fibers and Silica. **J Appl Polym Sci.** 120(6): 3242-3254.
- Lopattananon, N., K. Panawarangkul, K. Sahakaro and B. Ellis. 2006. Performance of Pineapple Leaf Fiber-Natural Rubber Composites: The Effect of Fiber Surface Treatments. **J Appl Polym Sci.** 102(2): 1974-1984.
- Lu, P. and Y.L. Hsieh. 2010. Preparation and Properties of Cellulose Nanocrystals: Rods, Spheres, and Network. **Carbohydr Polym.** 82(2): 329-336.
- Mandal, A. and D. Chakrabarty. 2011. Isolation of Nanocellulose from Waste Sugarcane Bagasse (Scb) and Its Characterization. **Carbohydr Polym.** 86(3): 1291-1299.
- Martinez-Sanz, M., A. Lopez-Rubio and J.M. Lagaron. 2011. Optimization of the Nanofabrication by Acid Hydrolysis of Bacterial Cellulose Nanowhiskers. **Carbohydr Polym.** 85(1): 228-236.
- Martins, I.M.G., S.P. Magina, L. Oliveira, C.S.R. Freire, A.J.D. Silvestre, C.P. Neto and A. Gandini. 2009. New Biocomposites Based on Thermoplastic Starch and Bacterial Cellulose. **Compos Sci Technol.** 69(13): 2163-2168.
- Mathew, L. 2009. **Development of Elastomeric Hybrid Composite Based on Synthesized Nanosilica and Short Nylon Fiber.** Ph.D. Thesis, Cochin University of Science and Technology.

- Mathew, L. and R. Joseph. 2007. Mechanical Properties of Short-Isora-Fiber-Reinforced Natural Rubber Composites: Effects of Fiber Length, Orientation, and Loading; Alkali Treatment; and Bonding Agent. **J Appl Polym Sci.** 103(3): 1640-1650.
- Muniandy, K., H. Ismail and O. N. 2011. Curing Characteristics and Mechanical Properties of Rattan Filled Natural Rubber Compounds. **Key Engineering Materials.** 471 - 472(845-850).
- Nickerson, R.F. and J.A. Habrle. 1947. Cellulose Intercrystalline Structure. **Ind. Eng. Chem.** 39(11): 1507–1512.
- Oksman, K., J.A. Etang, A.P. Mathew and M. Jonoobi. 2011. Cellulose Nanowhiskers Separated from a Bio-Residue from Wood Bioethanol Production. **Biomass Bioenerg.** 35(1): 146-152.
- Park, J.K., J.Y. Jung and T. Khan. 2009. Bacterial Cellulose, 724-739 pp. *In* G. O. Phillips and P. A. Williams. **Hand Book of Hydrocolloids.** Woodhead publishing limited United Kingdom.
- Pasquini, D., E.M. Teixeira, A.A.S. Curvelo, M.N. Belgacem and A. Dufresne. 2010. Extraction of Cellulose Whiskers from Cassava Bagasse and Their Applications as Reinforcing Agent in Natural Rubber. **Ind Crop Prod.** 32(486–490).
- Pecoraro, E., D. Manzani, Y. Messaddeq and S.J.L. Ribeiro. 2008. Bacterial Cellulose from Glucanacetobacter Xylinus: Preparation, Properties and Applications, 369-383 pp. *In* M. N. Belgacem and A. Gandini. **Monomers, Polymers and Composites from Renewable Resources.** Elsevier publications, The Netherlands.

Phisalaphong, M., T. Suwanmajo and P. Sangtherapitikul. 2008. Novel Nanoporous Membranes from Regenerated Bacterial Cellulose. **J Appl Polym Sci.** 107(1): 292–299.

Quéro, F. 2011. **Interfacial Micromechanics of Bacterial Cellulose Bio-Composites Using Raman Spectroscopy.** Ph.D. Thesis, The University of Manchester.

Rånby, B.G. 1952. The Cellulose Micelles. **Tappi.** 35(2): 53-58.

Rånby, B.G., A. Banderet and L.G. Sillén. 1949. Aqueous Colloidal Solutions of Cellulose Micelles **ACTA CHEM SCAND.** 3(649-650).

Rosa, M.F., E.S. Medeiros, J.A. Malmonge, K.S. Gregorski, D.F. Wood, L.H.C. Mattoso, G. Glenn, W.J. Orts and S.H. Imam. 2010. Cellulose Nanowhiskers from Coconut Husk Fibers: Effect of Preparation Conditions on Their Thermal and Morphological Behavior. **Carbohydr Polym.** 81(1): 83-92.

Sheykhnazari, S., T. Tabarsa, A. Ashori, A. Shakeri and M. Gholipour. 2011. Bacterial Synthesized Cellulose Nanofibers; Effects of Growth Times and Culture Mediums on the Structural Characteristics. **Carbohydr Polym.** 86(3): 1187-1191.

Siqueira, G., J. Bras and A. Dufresne. 2010a. Cellulosic Bionanocomposites: A Review of Preparation, Properties and Applications. **Polymer.** 2(728-765).

Siqueira, G., H. Abdillahi, J. Bras and A. Dufresne. 2010b. High Reinforcing Capability Cellulose Nanocrystals Extracted from *Syngonanthus Nitens* (Capim Dourado). **Cellulose.** 17(2): 289-298.

Siqueira, G., S. Tapin-Lingua, J. Bras, D.S. Perez and A. Dufresne. 2010c. Mechanical Properties of Natural Rubber Nanocomposites Reinforced with



Cellulosic Nanoparticles Obtained from Combined Mechanical Shearing, and Enzymatic and Acid Hydrolysis of Sisal Fibers. **Cellulose**. 18(57-65).

Srisuwan, L., K. Jarukumjorn and N. Suppakarn. 2011. Physical Properties of Rice Husk Fiber/Natural Rubber Composites. **Advanced Materials Research**. 410(90-93).

Staiger, M.P., H. Piao, S. Dean and P. Gostomski. 2007. Bacterial Cellulose Networks for Reinforcement of Polylactide, pp.1-9. *In* **16th International conference on composite materials**. Kyoto, Japan.

Teixeira, E.D., D. Pasquini, A.A.S. Curvelo, E. Corradini, M.N. Belgacem and A. Dufresne. 2009. Cassava Bagasse Cellulose Nanofibrils Reinforced Thermoplastic Cassava Starch. **Carbohydr Polym**. 78(3): 422-431.

Teixeira, E.D., T.J. Bondancia, K.B.R. Teodoro, A.C. Correa, J.M. Marconcini and L.H.C. Mattoso. 2011. Sugarcane Bagasse Whiskers: Extraction and Characterizations. **Ind Crop Prod**. 33(1): 63-66.

Trovatti, E., L.S. Serafim, C.S.R. Freire, A.J.D. Silvestre and C.P. Neto. 2011. Gluconacetobacter Sacchari: An Efficient Bacterial Cellulose Cell-Factory. **Carbohydr Polym**. 86(3): 1417-1420.

Trovatti, E., L. Oliveira, C.S.R. Freire, A.J.D. Silvestre, C.P. Neto, J.J.C.C. Pinto and A. Gandini. 2010. Novel Bacterial Cellulose-Acrylic Resin Nanocomposites. **Compos Sci Technol**. 70(7): 1148-1153.

Visakh, P.M., S. Thomas, K. Oksman and A.P. Mathew. 2012. Crosslinked Natural Rubber Nanocomposites Reinforced with Cellulose Whiskers Isolated from Bamboo Waste: Processing and Mechanical/Thermal Properties. **Compos Part a-Appl S**. 43(4): 735-741.

- Wan, Y.Z., H.L. Luo, F. He, H. Liang, Y. Huang and X.L. Li. 2009. Mechanical, Moisture Absorption, and Biodegradation Behaviours of Bacterial Cellulose Fibre-Reinforced Starch Biocomposites. **Compos Sci Technol.** 69(7-8): 1212-1217.
- Wang, N., E.Y. Ding and R.S. Cheng. 2007. Thermal Degradation Behaviors of Spherical Cellulose Nanocrystals with Sulfate Groups. **Polymer.** 48(12): 3486-3493.
- Watanabe, K., M. Tabuchi, Y. Morinaga and F. Yoshinaga. 1998. Structural Features and Properties of Bacterial Cellulose Produced in Agitated Culture. **Cellulose.** 5(3): 187-200.
- Woehl, M.A., C.D. Canestraro, A. Mikowski, M.R. Sierakowski, L.P. Ramos and F. Wypych. 2010. Bionanocomposites of Thermoplastic Starch Reinforced with Bacterial Cellulose Nanofibres: Effect of Enzymatic Treatment on Mechanical Properties. **Carbohydr Polym.** 80(3): 866-873.
- Wongsorat, W., N. Suppakarn and K. Jarukumjorn. 2011. Sisal Fiber/Natural Rubber Composites: Effect of Fiber Content and Interfacial Modification. **Advanced Materials Research.** 410(63-66).
- Yoshinaga, F., N. Tonouchi and K. Watanabe. 1997. Research Progress in Production of Bacterial Cellulose by Aeration and Agitation Culture and Its Application as a New Industrial Material. **Biosci. Biotech. Biochem.** 16(2): 219-224.
- Zhang, Y.D., Q.F. Liu, Q.A. Zhang and Y.P. Lu. 2010. Gas Barrier Properties of Natural Rubber/Kaolin Composites Prepared by Melt Blending. **Appl Clay Sci.** 50(2): 255-259.

**CIRRICULUM VITAE**

NAME : Ms. Walaiporn Rungjang

BIRTH DATE : March 27, 1986

BIRTH PLACE :Kumpangpet, Thailand

EDUCATION	: <u>YEAR</u>	<u>INSTITUTE</u>	<u>DEGREE/DIPLOMA</u>
	2008	KMUTNB	B.S.(Agro-Industry technology and management)

POSITION/TITLE : Master Student

WORK PLACE : Department of Biotechnology, Agro-Industry Building 3,  
Faculty of Agro-Industry, Kasetsart University